THE TOP QUARK

Updated September 2013 by T.M. Liss (Univ. Illinois), F. Maltoni (Univ. Catholique de Louvain), and A. Quadt (Univ. Göttingen).

A. Introduction

The top quark is the $Q = 2/3$, $T_3 = +1/2$ member of the weak-isospin doublet containing the bottom quark (see the review on the "Electroweak Model and Constraints on New Physics" for more information). Its phenomenology is driven by its large mass. Being heavier than a W boson, it is the only quark that decays semi-weakly, i.e., into a real W boson and a b quark, before hadronization can occur. In addition, it is the only quark whose Yukawa coupling to the Higgs boson is order of unity. For these reasons the top quark plays a special role in the Standard Model (SM) and in many extensions thereof. An accurate knowledge of its properties (mass, couplings, production cross section, decay branching ratios, *etc.*) can bring key information on fundamental interactions at the electroweak breaking scale and beyond. This review provides a concise discussion of the experimental and theoretical issues involved in the determination the top-quark properties.

B. Top-quark production at the Tevatron and LHC

In hadron collisions, top quarks are produced dominantly in pairs through the processes $q\overline{q} \to t\overline{t}$ and $gg \to t\overline{t}$, at leading order in QCD. Approximately 85% of the production cross section at the Tevatron is from $q\overline{q}$ annihilation, with the remainder from gluon-gluon fusion, while at LHC energies about 90% of the production is from the latter process at $\sqrt{s} = 14$ TeV ($\approx 80\%$ at $\sqrt{s} = 7$ TeV).

Predictions for the total cross sections are now available at next-to-next-to leading order (NNLO) with next-to-next-to-leading-log (NNLL) soft gluon resummation [1]. These results supersede previous approximated ones [2]. Assuming a top-quark mass of 173.3 GeV/c^2, close to the world average [3](LHC results not yet included), the resulting theoretical prediction of the top-quark pair cross-section at NNLO+NNLL accuracy at the Tevatron at $\sqrt{s} = 1.96$ TeV is $\sigma_{t\bar{t}} = 7.164^{+0.11+0.17}_{-0.20-0.12}$ pb

where the first uncertainty is from scale dependence and the second from parton distribution functions, while at the LHC at $\sqrt{s}$ = 7 TeV (8 TeV) is $\sigma_{t\bar{t}} = 172.0^{+4.4+4.7}_{-5.8-4.8}$ pb ($\sigma_{t\bar{t}} = 245.8^{+6.2+6.2}_{-8.4-6.4}$ pb).

Electroweak single top-quark production mechanisms, namely from $q\overline{q}' \to t\overline{b}$ [4], $qb \to q't$ [5], mediated by virtual s-channel and t-channel W-bosons, and Wt-associated production, through $bg \to W^-t$, lead to somewhat smaller cross sections. For example, t-channel production, while suppressed by the weak coupling with respect to the strong pair production, is kinematically enhanced, resulting in a sizable cross section both at Tevatron and LHC energies. At the Tevatron, the t- and s-channel cross sections of top and antitop are identical, while at the LHC they are not. Approximate NNLO cross sections for t-channel single top-quark production ($t + \bar{t}$) are calculated for m_t = 173.3 GeV/c^2 to be $2.06^{+0.13}_{-0.13}$ pb in $p\overline{p}$ collisions at $\sqrt{s}$ = 1.96 TeV (scale and parton distribution functions uncertainties are combined in quadrature) and $65.7^{+1.9}_{-1.9}$ ($87.1^{+0.24}_{-0.24}$) pb in pp collisions at $\sqrt{s}$ = 7 (8) TeV, where 65% and 35% are the relative proportions of t and $\bar{t}$ [6]. For the s-channel, these calculations yield $1.03^{+0.05}_{-0.05}$ pb for the Tevatron, and $4.5^{+0.2}_{-0.2}(5.5^{+0.2}_{-0.2})$ pb for $\sqrt{s}$ = 7 (8) TeV at the LHC, with 69% (31%) of top (anti-top) quarks [7]. While negligible at the Tevatron, at LHC energies the Wt-associated production becomes relevant. At $\sqrt{s}$ = 7 (8) TeV, an approximate NNLO calculation using the MSTW2008 PDF gives $15.5^{+1.2}_{-1.2}(22.1^{+1.5}_{-1.5})$ pb ($t + \bar{t}$), with an equal proportion of top and anti-top quarks [8].

Assuming $|V_{tb}| \gg |V_{td}|, |V_{ts}|$ (see the review "The CKM Quark-Mixing Matrix" for more information), the cross sections for single top production are proportional to $|V_{tb}|^2$, and no extra hypothesis is needed on the number of quark families or on the unitarity of the CKM matrix in extracting $|V_{tb}|$. Separate measurements of the s- and t-channel processes provide sensitivity to physics beyond the Standard Model [9].

With a mass above the Wb threshold, and $|V_{tb}| \gg |V_{td}|, |V_{ts}|$, the decay width of the top quark is expected to be dominated by the two-body channel $t \to Wb$. Neglecting terms of order

m_b^2/m_t^2, α_s^2, and $(\alpha_s/\pi)M_W^2/m_t^2$, the width predicted in the SM at NLO is [10]:

$$\Gamma_t = \frac{G_F m_t^3}{8\pi\sqrt{2}} \left(1 - \frac{M_W^2}{m_t^2}\right)^2 \left(1 + 2\frac{M_W^2}{m_t^2}\right) \left[1 - \frac{2\alpha_s}{3\pi}\left(\frac{2\pi^2}{3} - \frac{5}{2}\right)\right], \quad (1)$$

where m_t refers to the top-quark pole mass. The width for a value of $m_t = 173.3$ GeV/c^2 is 1.35 GeV/c^2 (we use $\alpha_s(M_Z) = 0.118$) and increases with mass. With its correspondingly short lifetime of $\approx 0.5 \times 10^{-24}$ s, the top quark is expected to decay before top-flavored hadrons or $t\bar{t}$-quarkonium-bound states can form [11]. In fact, since the decay time is close to the would-be-resonance binding time, a peak will be visible in e^+e^- scattering at the $t\bar{t}$ threshold [12] and it is in principle present (yet very difficult to measure) in hadron collisions, too [13]. The order α_s^2 QCD corrections to Γ_t are also available [14], thereby improving the overall theoretical accuracy to better than 1%.

The final states for the leading pair-production process can be divided into three classes:

A. $t\bar{t} \to W^+ b\, W^- \bar{b} \to q\,\overline{q}'\, b\, q''\,\overline{q}'''\,\bar{b}$, (45.7%)

B. $t\bar{t} \to W^+ b\, W^- \bar{b} \to q\,\overline{q}'\, b\, \ell^-\,\overline{\nu}_\ell\,\bar{b} + \ell^+\,\nu_\ell\, b\, q''\,\overline{q}'''\,\bar{b}$, (43.8%)

C. $t\bar{t} \to W^+ b\, W^- \bar{b} \to \overline{\ell}\,\nu_\ell\, b\, \ell'\,\overline{\nu}_{\ell'}\,\bar{b}$. (10.5%)

The quarks in the final state evolve into jets of hadrons. A, B, and C are referred to as the all-jets, lepton+jets (ℓ+jets), and dilepton ($\ell\ell$) channels, respectively. Their relative contributions, including hadronic corrections, are given in parentheses assuming lepton universality. While ℓ in the above processes refers to e, μ, or τ, most of the analyses distinguish the e and μ from the τ channel, which is more difficult to reconstruct. Therefore, in what follows, we will use ℓ to refer to e or μ, unless otherwise noted. Here, typically leptonic decays of τ are included. In addition to the quarks resulting from the top-quark decays, extra QCD radiation (quarks and gluons) from the colored particles in the event can lead to extra jets.

The number of jets reconstructed in the detectors depends on the decay kinematics, as well as on the algorithm for reconstructing jets used by the analysis. Information on the transverse momenta of neutrinos is obtained from the imbalance

in transverse momentum measured in each event (missing p_T, which is here also called missing E_T).

The identification of top quarks in the electroweak single top channel is much more difficult than in the QCD $t\bar{t}$ channel, due to a less distinctive signature and significantly larger backgrounds, mostly due to $t\bar{t}$ and W+jets production.

Fully exclusive predictions via Monte Carlo generators for the $t\bar{t}$ and single top production processes at NLO accuracy in QCD, including top-quark decays, are available [15,16] through the `MC@NLO` [17] and `POWHEG` [18] methods.

Besides fully inclusive QCD or EW top-quark production, more exclusive final states can be accessed at hadron colliders, whose cross sections are typically much smaller, yet can provide key information on the properties of the top quark. For all relevant final states (*e.g.*, $t\bar{t}\gamma, t\bar{t}Z, t\bar{t}W, t\bar{t}H, t\bar{t}$+jets, $t\bar{t}b\bar{b}, t\bar{t}t\bar{t}$) automatic or semi-automatic predictions at NLO accuracy in QCD also in the form of event generators, *i.e.*, interfaced to parton-shower programs, are available (see the review "Monte Carlo event generators" for more information).

C. Top-quark measurements

Since the discovery of the top quark, direct measurements of $t\bar{t}$ production have been made at four center-of-mass energies, providing stringent tests of QCD. The first measurements were made in Run I at the Tevatron at $\sqrt{s} = 1.8$ TeV. In Run II at the Tevatron relatively precise measurements were made at $\sqrt{s} = 1.96$ TeV. Finally, beginning in 2010, measurements have been made at the LHC at $\sqrt{s} = 7$ TeV and $\sqrt{s} = 8$ TeV.

Production of single top quarks through electroweak interactions has now been measured with good precision at the Tevatron at $\sqrt{s} = 1.96$ TeV, and at the LHC at both $\sqrt{s} = 7$ TeV and $\sqrt{s} = 8$ TeV. Recent measurements at the Tevatron are beginning to separate the s- and t-channel production cross sections, and at the LHC, the Wt mechanism as well, though the t-channel is measured with best precision to date. The measurements allow an extraction of the CKM matrix element V_{tb}.

The top-quark mass is now measured at the 0.5% level, by far the most precisely measured quark mass. Together with the

W-boson mass measurement and the newly discovered Higgs boson, this provides a stringent test of the Standard Model.

With almost 9 fb^{-1} of Tevatron data analyzed as of this writing, and almost 20 fb^{-1} of LHC data, many properties of the top quark are now being measured with precision. These include properties related to the production mechanism, such as $t\bar{t}$ spin correlations, forward-backward or charge asymmetries, and differential production cross sections, as well as properties related to the $t-W-b$ decay vertex, such as the helicity of the W-bosons from the top-quark decay. In addition, many searches for physics beyond the Standard Model are being performed with increasing reach in both production and decay channels.

In the following sections we review the current status of measurements of the characteristics of the top quark.

C.1 Top-quark production

C.1.1 $t\bar{t}$ production: Fig. 1 summarizes the $t\bar{t}$ production cross-section measurements from both the Tevatron and LHC. The most recent measurement from DØ [19], combining the measurements from the dilepton and lepton plus jets final states in 5.4 fb^{-1}, is $7.56^{+0.63}_{-0.56}$ pb. From CDF the most precise measurement made recently [20] is in 4.6 fb^{-1} and is a combination of dilepton, lepton plus jets, and all-hadronic final-state measurements, yielding 7.50 ± 0.48 pb. Both of these measurements assume a top-quark mass of 172.5 GeV/c^2. The dependence of the cross section measurements on the value chosen for the mass is less than that of the theory calculations because it only affects the determination of the acceptance. In some analyses also the shape of topological variables might be modified. Very recently, CDF updated some of their measurements with the full Run-II dataset up to 8.8 fb^{-1}. The resulting combined $t\bar{t}$ cross-section is $\sigma_{t\bar{t}} = 7.63 \pm 0.50$ pb (7.1%) for CDF, $\sigma_{t\bar{t}} = 7.56 \pm 0.59$ pb (9.3%) for DØ and $\sigma_{t\bar{t}} = 7.60 \pm 0.41$ pb (5.4%) for the Tevatron combination [21] in good agreement with the SM expectation of $7.16^{+0.20}_{-0.23}$ pb at NNLO+NNLL in perturbative QCD. The contributions to the uncertainty are 0.20 pb from statistical sources, 0.29 pb from systematic sources, and 0.21 pb from the uncertainty on the integrated luminosity.

CDF also performs measurements of the $t\bar{t}$ production cross section normalized to the Z production cross section in order to reduce the impact of the luminosity uncertainty.

The LHC experiments ATLAS and CMS use similar techniques to measure the $t\bar{t}$ cross-section in pp collisions. At $\sqrt{s} = 7$ TeV, ATLAS performs measurements in 0.7 fb^{-1} in the lepton+jets channel [22], in the dilepton channel [23], and in 1.02 fb^{-1} in the all-hadronic channel [24], which together yield a combined value of $\sigma_{t\bar{t}} = 177 \pm 3(stat.)^{+8}_{-7}(syst.) \pm 7(lumi.)$ pb (6.2%) assuming $m_t = 172.5$ GeV/c^2 [25]. Further analyses in the hadronic tau plus jets channel in 1.67 fb^{-1} [26], the hadronic tau + lepton channel in 2.05 fb^{-1} [27], and the all-hadronic channel in 4.7 fb^{-1} [28] yield consistent albeit less precise results. CMS performs $t\bar{t}$ cross-section measurements with 2.3 fb^{-1} in the e/μ+jets channel [29] and in the dilepton channel [30], with 3.5 fb^{-1} in the all-hadronic channel [31], with 2.2 fb^{-1} in the lepton+τ channel [32], and with 3.9 fb^{-1} in the τ+jets channel [33]. The most precise result is obtained in the dilepton channel, where they obtain $\sigma_{t\bar{t}} = 162 \pm 2(stat.) \pm 5(syst.) \pm 4(lumi.)$ pb, which corresponds to a 4.2% precision [30].

At $\sqrt{s} = 8$ TeV, ATLAS and CMS perform cross-section analyses as well, although only a few channels have been considered so far due to the large number of systematic uncertainties being dominant. ATLAS measures the $t\bar{t}$ cross-section in the lepton+jets channel with 5.8 fb^{-1} [34], and in the $e\mu$ dilepton channel using 20.3 fb^{-1} [35]. In the latter, they select an extremely clean sample and determine the $t\bar{t}$ cross-section simultaneously with the efficiency to reconstruct and b-tag jets, yielding $\sigma_{t\bar{t}} = 237.7 \pm 1.7(stat.) \pm 7.4(syst.) \pm 7.4(lumi.) \pm 4.0(beam\,energy)$ pb assuming $m_t = 172.5$ GeV/c^2, which corresponds to a 4.7% precision. CMS performs a template fit to the M_{lb} mass distribution using 2.7 fb^{-1} in the lepton+jets channel [36] and a cut-and-count analysis in 2.4 fb^{-1} in the dilepton channel [37]. In combination, they achieve $\sigma_{t\bar{t}} = 227 \pm 3(stat.) \pm 11(syst.) \pm 10(lumi.)$ pb for $m_t = 172.5$ GeV/c^2 [37], which corresponds to a 6.7% precision.

These experimental results should be compared to the theoretical calculations that yield $7.16^{+0.20}_{-0.23}$ pb for top-quark mass of 173.3 GeV/c^2 [1] at $\sqrt{s} = 1.96$ TeV, $\sigma_{t\bar{t}} = 172.0^{+6.4}_{-7.5}$ pb at $\sqrt{s} = 7$ TeV, and $\sigma_{t\bar{t}} = 245.8^{+8.8}_{-10.6}$ pb at $\sqrt{s} = 8$ TeV, at the LHC [1](see Section B).

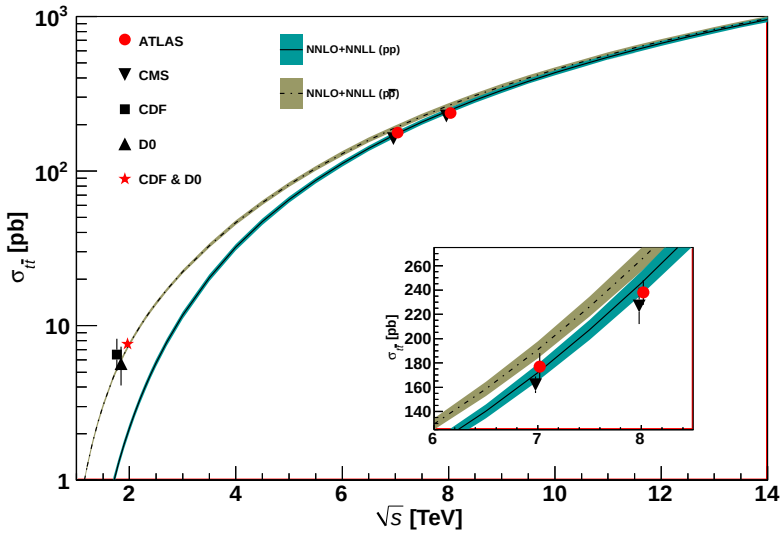

Figure 1: Measured and predicted $t\bar{t}$ production cross sections from Tevatron energies in $p\overline{p}$ collisions to LHC energies in pp collisions. Tevatron data points at $\sqrt{s} = 1.8$ TeV are from Refs. [41,42]. Those at $\sqrt{s} = 1.96$ TeV are from Refs. [19–21]. The ATLAS and CMS data points are from Refs. [25,35] and [30,36,37], respectively. Theory curves are generated using [1] for $m_t = 173.3$ GeV/c^2. Figure adapted from Ref. [40].

In Fig. 1, one sees the importance of $p\overline{p}$ at Tevatron energies where the valence antiquarks in the antiprotons contribute to the dominant $q\overline{q}$ production mechanism. At LHC energies, the dominant production mode is gluon-gluon fusion and the pp-$p\overline{p}$ difference nearly disappears. The excellent agreement of these measurements with the theory calculations is a strong validation of QCD and the soft-gluon resummation techniques employed in the calculations. The measurements reach high precision and provide stringent tests of pQCD calculations at NNLO+NNLL level including their respective PDF uncertainties.

Most of these measurements assume a $t \to Wb$ branching ratio of 100%. CDF and DØ have made direct measurements

of the $t \to Wb$ branching ratio [38]. Comparing the number of events with 0, 1 and 2 tagged b jets in the lepton+jets channel, and also in the dilepton channel, using the known b-tagging efficiency, the ratio $R = B(t \to Wb)/\sum_{q=d,s,b} B(t \to Wq)$ can be extracted. In 5.4 fb^{-1} of data, DØ measures $R = 0.90 \pm 0.04$, 2.5σ from unity. A similar measurement was made by CMS in 16.7 fb^{-1} at $\sqrt{s} = 8$ TeV. They find $R = 1.023^{+0.036}_{-0.034}$ and $R > 0.945$ at 95% C.L. [39]. A significant deviation of R from unity would imply either non-SM top-quark decay (for example a flavor-changing neutral-current decay), or a fourth generation of quarks.

Thanks to the large available event samples, the Tevatron and the LHC experiments performed first differential cross-section measurements in $t\bar{t}$ production. Such measurements are crucial, as they allow even more stringent tests of perturbative QCD as description of the production mechanism, allow the extraction or the use of PDF fits, and enhance the sensitivity to possible new physics contributions. Furthermore, such measurements reduce the uncertainty in the description of $t\bar{t}$ production as background in Higgs physics and searches for rare processes or beyond Standard Model physics. Differential cross-sections are typically measured by a selection of candidate events, their kinematic reconstruction and subsequent unfolding of the obtained event counts in bins of kinematic distributions in order to correct for detector resolution effects, acceptance and migration effects. In some cases a bin-by-bin unfolding is used, other analyses use a more sophisticated technique, taking into account the known migrations effects and correlations or employing some regularization.

Using 2.7 fb^{-1}, CDF measured the differential cross-section with respect to the $t\bar{t}$ invariant mass, $d\sigma/dM_{t\bar{t}}$, in the lepton+jets channel providing sensitivity to a variety of exotic particles decaying into $t\bar{t}$ pairs [43]. In 9.7 fb^{-1} of lepton+jets data, DØ measured the differential $t\bar{t}$ production cross-section with respect to the transverse momentum and absolute rapidity of the top quarks as well as of the invariant mass of the $t\bar{t}$ pair [44], which are all found to be in good agreement

with the SM predictions. Also ATLAS measured the differential $t\bar{t}$ production cross-section with respect to the top-quark transverse momentum, and of the mass, transverse momentum and rapidity of the $t\bar{t}$ system in 4.6 fb^{-1} at $\sqrt{s} = 7$ TeV in the lepton+jets channel [45]. The measured spectra are fully corrected for detector efficiency and resolution effects and are compared to several Monte Carlo simulations as well as selected theoretical calculations. The results show sensitivity to these predictions and to different sets of parton distribution functions. It is found that data is softer than all predictions in the tail of the top-quark p_T spectrum beginning at 200 GeV, particularly in the case of the `Alpgen`+`Herwig` generator. The $m_{t\bar{t}}$ spectrum is not well described by NLO+NNLL calculations and there are also disagreements between the measured $y_{t\bar{t}}$ spectrum and the `MC@NLO`+`Herwig` and `POWHEG`+`Herwig` generators, both evaluated with the CT10 PDF set. All distributions show a preference for HERAPDF1.5 when used for the NLO QCD predictions. In 5.0 fb^{-1} of $\sqrt{s} = 7$ TeV data in the lepton+jets and the dilepton channels, CMS measured normalised differential $t\bar{t}$ cross-sections with respect to kinematic properties of the final-state charged leptons and jets associated to b-quarks, as well as those of the top quarks and the $t\bar{t}$ system. The data are compared with several predictions from perturbative QCD calculations and found to be consistent [46]. Recently, in 12 fb^{-1} at $\sqrt{s} = 8$ TeV, CMS repeated those measurements in the lepton+jets [47] and in the dilepton channels [48]. While the overall precision is improved, no significant deviations from the Standard Model are observed. Very recently, they also performed a normalized differential cross-section measurement in 20 fb^{-1} of lepton+jets data with respect to a number of event-level observables, including missing transverse energy, jet transverse momentum scalar sum, total event transverse momentum scalar sum, leptonic W transverse momentum, and leptonic W transverse mass. The results are consistent with the Standard Model expectations [49].

Further cross-section measurements are performed for $t\bar{t}$+heavy flavour and $t\bar{t}$+jets production [50,51].

C.1.2 Single-top production: Single-top quark production was first observed in 2009 by DØ [52] and CDF [53,54] at the Tevatron. The production cross section at the Tevatron is roughly half that of the $t\bar{t}$ cross section, but the final state with a single W-boson and typically two jets is less distinct than that for $t\bar{t}$ and much more difficult to distinguish from the background of W+jets and other sources. A recent review of the first observation and the techniques used to extract the signal from the backgrounds can be found in [55].

The dominant production at the Tevatron is through s-channel and t-channel W-boson exchange. Associated production with a W-boson (Wt production) has a cross section that is too small to observe at the Tevatron. The t-channel process is $qb \to q't$, while the s-channel process is $q\overline{q'} \to t\bar{b}$. The s- and t-channel productions can be separated kinematically. This is of particular interest because potential physics beyond the Standard Model, such as fourth-generation quarks, heavy W and Z bosons, flavor-changing-neutral-currents [9], or a charged Higgs boson, would affect the s- and t-channels differently. However, the separation is difficult and initial observations and measurements at the Tevatron by both experiments were of combined $s+t$-channel production. The two experiments combined their measurements for maximum precision with a resulting $s+t$ channel production cross section of $2.76^{+0.58}_{-0.47}$ pb [56]. The measured value assumes a top-quark mass of 170 GeV/c^2. The mass dependence of the result comes both from the acceptance dependence and from the $t\bar{t}$ background evaluation. Also the shape of discriminating topological variables is sensitive to m_t. It is therefore not necessarily a simple linear dependence but amounts to only a few tenths of picobarns over the range $170 - 175$ GeV/c^2. The measured value agrees well with the theoretical calculation at $m_t = 173$ GeV/c^2 of $\sigma_{s+t} = 3.12$ pb (including both top and anti-top production) [6,7].

Recently, CDF has updated the $s+t$-channel measurement with 7.5 fb^{-1} to $\sigma_{s+t} = 3.04^{+0.57}_{-0.53}$ pb assuming a Standard Model ratio of s- to t-channel, resulting in a lower limit of $|V_{tb}| > 0.78$ at 95% C.L. [57]. They also analyzed the full Run-II data set of 9.1 fb^{-1} in W+jets events where no electron

or muon has been identified, and where the tau lepton in the $t \to Wb \to \tau\nu b$ channel is reconstructed as a jet in the calorimeters. Multivariate analysis discriminants and a profile likelihood technique are used to obtain a cross section of $\sigma_{s+t} = 3.0^{+1.5}_{-1.4}$ pb [58]. DØ has measured the combined cross section to $\sigma_{s+t} = 3.43^{+0.73}_{-0.74}$ pb for $m_t = 172.5/c^2$ GeV [59].

Both experiments have done separate measurements of the s- and t-channel cross sections by reoptimizing the analysis for one or both of the channels separately. In a simultaneous measurement of s- and t-channel cross sections, CDF measures $\sigma_s = 1.81^{+0.63}_{-0.58}$ pb and $\sigma_t = 1.49^{+0.47}_{-0.42}$ pb, respectively, in 7.5 fb^{-1} of data [57]. Using 9.4 fb^{-1}, they performed an analysis in the missing E_T plus $b\bar{b}$ channel yielding $\sigma_s = 1.10^{+0.65}_{-0.66}$ pb [58,60] and in the $l\nu b\bar{b}$ channel resulting in $\sigma_s = 1.43^{+0.44}_{-0.42}$ pb [61]. The latter also corresponds to a 3.7 standard deviations evidence. In this analysis, CDF assumes the t-channel cross-section to take the SM value. DØ performs a sophisticated multivariate analysis combining a matrix-element technique, a Bayesian neural network and boosted decision tress to form one output variable using another boosted decision tree. In 9.7 fb^{-1} of integrated luminosity, they measure $\sigma_s = 1.10^{+0.33}_{-0.31}$ pb [62], which corresponds to 3.7 standard deviations and is the first evidence for s-channel single-top production at the Tevatron. In this measurement, they also obtain $\sigma_t = 3.07^{+0.53}_{-0.49}$ pb, which corresponds to 7.7 standard deviations. In combination, the result is $\sigma_{s+t} = 4.11^{+0.60}_{-0.55}$ pb [62]. In this measurement, they do not make any assumption about the t-channel. They also set a limit on $|V_{tb}| > 0.92$ at 95% C.L. In a slightly different analysis, using 5.4 fb^{-1}, they measure the t-channel production cross section in a dedicated analysis [59,63] with a significance of 5.5 standard deviations using a variety of advanced analysis techniques similar to those described in [55]. These take advantage of kinematic differences in such things as the leading b-tagged jet p_T, centrality of jets, lepton charge times η of the jets, and the scalar sum of the energy of the final state objects. The $p\overline{p} \to tq + X$ cross section is measured to be 2.90 ± 0.59 pb, assuming a top-quark mass of 172.5 GeV/c^2. This is in good agreement with the theoretical value at this

mass of 2.08 ± 0.13 pb [6]. It should be noted that the theory citations here list cross sections for t or $\overline{t}$ alone, whereas the experiments measure the sum. At the Tevatron, these cross sections are equal. The theory values quoted here already include this factor of two.

The Tevatron experiments are working on an s-channel combination, which is expected to come out very soon.

At the LHC, the t-channel cross section is expected to be more than three times as large as s-channel and Wt production, combined. Both ATLAS and CMS have measured single top production cross sections at $\sqrt{s} = 7$ TeV in pp collisions (assuming $m_t = 172.5$ GeV/c^2 unless noted otherwise), where they recently observed t-channel production [64,65]. ATLAS analyses 1.04 fb^{-1} of 7 TeV data in the lepton plus 2 or 3 jets channel with one b-tag by fitting the distribution of a multivariate discriminant constructed with a neural network, yielding $\sigma_t = 83 \pm 4(stat.)^{+20}_{-19}(syst)$ pb (this value refers to the sum of top and antitop cross-section) as well as $|V_{tb}| = 1.13^{+0.14}_{-0.13}$ and $|V_{tb}| > 0.75$ at 95% C.L. [64]. In an update with 4.7 fb^{-1} using a binned maximum likelihood fit to the output distribution of neural networks, they find $\sigma_t = 53.2 \pm 10.8$ pb and $\sigma_{\bar{t}} = 29.5^{+7.4}_{-7.5}$ pb with a cross-section charge ratio $R_t = 1.81^{+0.23}_{-0.22}$ [66] that is sensitive to the ratio of the up-quark and down-quark parton distribution functions in the proton. CMS follows two approaches in 1.6 fb^{-1} of lepton plus jets events. The first approach exploits the distributions of the pseudorapidity of the recoil jet and reconstructed top-quark mass using background estimates determined from control samples in data. The second approach is based on multivariate analysis techniques that probe the compatibility of the candidate events with the signal. They find $\sigma_t = 67.2 \pm 6.1$ pb, and $|V_{tb}| = 1.020 \pm 0.046(meas.) \pm 0.017(theor.)$ [65].

At $\sqrt{s} = 8$ TeV, both experiments repeat and refine their measurements. ATLAS uses 5.8 fb^{-1} by performing a combined binned maximum likelihood fit to the neural network output distribution. The measured t-channel cross-section is $\sigma_t = 95.1 \pm 2.4(stat.) \pm 18.0(syst.)$ pb with $|V_{tb}| = 1.04^{+0.1}_{-0.11}$ and $|V_{tb}| > 0.80$

at 95% C.L. [67]. CMS uses 5.0 fb^{-1} in the muon plus jets channel, exploiting the pseudorapidity distribution of the recoil jet. They find $\sigma_t = 80.1 \pm 5.7(stat.) \pm 11.0(syst.) \pm 4.0(lumi)$ pb [68] assuming $m_t = 173$ GeV/c^2. A combination of the two measurements yields $\sigma_t = 85 \pm 4(stat.) \pm 11(syst.) \pm 3(lumi.)$ pb [69]. Very recently, CMS has updated their measurement with the complete Run-I dataset of 20 fb^{-1} and furthermore measured the top-quark polarization in t-channel single top production to be $P_t = 0.82 \pm 0.12(stat.) \pm 0.32(syst.)$, which is consistent with the SM expectation [70]. Based on 12.2 fb^{-1}, CMS updated their results to find $\sigma_t = 49.9 \pm 9.1$ pb and $\sigma_{\bar{t}} = 28.3 \pm 5.5$ pb, which yields a cross-section charge ratio of $R_t = 1.76 \pm 0.27$ for $m_t = 173$ GeV/c^2 in agreement with the Standard Model [71].

The s-channel production cross section is expected to be only 4.6 ± 0.3 pb for $m_t = 173$ GeV/c^2 at $\sqrt{s} = 7$ TeV [7], and has not yet been observed at LHC. The Wt process has a theoretical cross section of 15.6 ± 1.2 pb [8]. This is of interest because it probes the $W - t - b$ vertex in a different kinematic region than s- and t-channel production, and because of its similarity to the associated production of a charged-Higgs boson and a top quark. The signal is difficult to extract because of its similarity to the $t\bar{t}$ signature. Furthermore, it is difficult to uniquely define because at NLO a subset of diagrams have the same final state as $t\bar{t}$ and the two interfere [72]. The cross section is calculated using the *diagram removal* technique [73] to define the signal process. In the diagram removal technique the interfering diagrams are removed, at the amplitude level, from the signal definition (an alternate technique, *diagram subtraction* removes these diagrams at the cross-section level and yields similar results). These techniques work provided the selection cuts are defined such that the interference effects are small, which is usually the case.

Both, ATLAS and CMS, also provide evidence for the associate Wt production at $\sqrt{s} = 7$ TeV [74,75]. ATLAS uses 2.05 fb^{-1} in the dilepton plus missing E_T plus jets channel, where a template fit to the final classifier distributions resulting from boosted decision trees as signal to background separation

is performed. The result is incompatible with the background-only hypothesis at the 3.3σ (3.4σ expected) level, yielding $\sigma_{Wt} = 16.8 \pm 2.9(stat.) \pm 4.9(syst.)$ pb and $|V_{tb}| = 1.03^{+0.16}_{-0.19}$ [74]. CMS uses 4.9 fb^{-1} in the dilepton plus jets channel with at least one b-tag. A multivariate analysis based on kinematic properties is utilized to separate the $t\bar{t}$ background from the signal. The observed signal has a significance of 4.0σ and corresponds to a cross section of $\sigma_{Wt} = 16^{+5}_{-4}$ pb [75]. Both experiments repeated their analyses at $\sqrt{s} = 8$ TeV. ATLAS uses 20.3 fb^{-1} to select events with one electron and one oppositely-charged muon, significant missing transverse momentum and at least one b-tagged central jet. They perform a template fit to a boosted decision tree classifier distribution and obtain $\sigma_{Wt} = 27.2 \pm 5.8$ pb and $|V_{tb}| = 1.10 \pm 0.12(exp.) \pm 0.03(theory)$ [76], which corresponds to a 4.2σ significance. Assuming $|V_{tb}| \gg |V_{ts}|, |V_{td}|$ they derive $|V_{tb}| > 0.72$ at 95% C.L. CMS uses 12.2 fb^{-1} in events with two leptons and a jet originated from a b-quark. A multivariate analysis based on kinematic properties is utilized to separate the signal and background. The Wt associate production signal is observed at the level of 6.0σ, yielding $\sigma_{Wt} = 23.4^{+5.5}_{-5.4}$ pb and $|V_{tb}| = 1.03 \pm 0.12(exp.) \pm 0.04(theory)$ [77].

At ATLAS, a search for s-channel single top quark production is performed in 0.7 fb^{-1} using events containing one lepton, missing transverse energy and two b-jets. Using a cut-based analysis, an observed (expected) upper limit at 95% C.L. on the s-channel cross-section of $\sigma_s < 26.5(20.5)$ pb is obtained [78].

Fig. 2 provides a summary of all single top cross-section measurements at the Tevatron and the LHC as a function of the center-of-mass energy. All cross-section measurements are very well described by the theory calculation within their uncertainty.

C.1.3 Top-Quark Forward-Backward & Charge Asymmetry: A forward-backward asymmetry in $t\bar{t}$ production arises from an interference between the Born and box production diagrams and between diagrams with initial- and final-state gluon

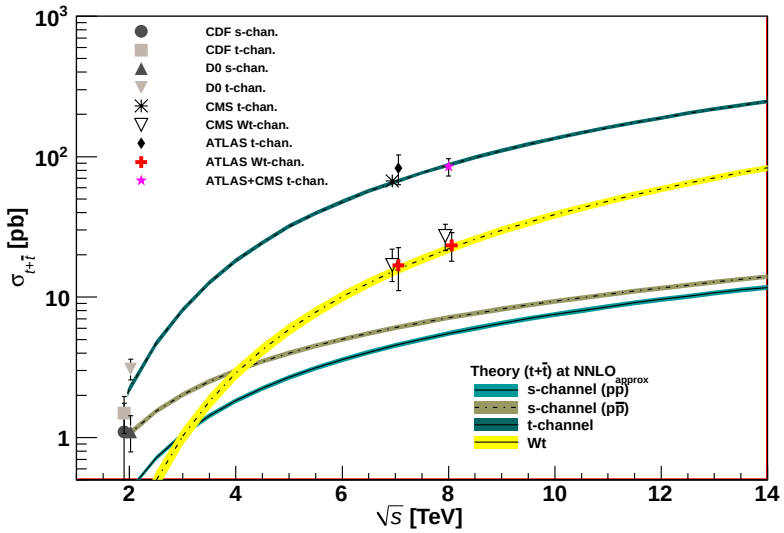

Figure 2: Measured and predicted single top production cross sections from Tevatron energies in $p\overline{p}$ collisions to LHC energies in pp collisions. Tevatron data points at $\sqrt{s} = 1.96$ TeV are from Refs. [57,60] and [62]. The ATLAS and CMS data points at $\sqrt{s} = 7$ TeV are from Refs. [64,66,74,78] and [79,65,75], respectively. The ones at $\sqrt{s} = 8$ TeV are from Refs. [67,69,76] and [68,69,77]. Theory curves are generated using [6,7,8].

radiation. The asymmetry, A_{FB}, is defined by

$$A_{FB} = \frac{N(\Delta y > 0) - N(\Delta y < 0)}{N(\Delta y > 0) + N(\Delta y < 0)} \tag{2}$$

where $\Delta y = y_t - y_{\bar{t}}$ is the rapidity difference between the top- and the anti-top quark. NLO calculations predict a small A_{FB} at the Tevatron. The most recent calculations at NLO, including electromagnetic and electroweak corrections, yield a predicted asymmetry of $(\approx 8.8 \pm 0.6)\%$ [80,81].

Both, CDF and DØ, have measured asymmetry values in excess of the SM prediction, fueling speculation about exotic production mechanisms (see, for example, [82] and references therein). The first measurement of this asymmetry by DØ in 0.9 fb^{-1} [83] found an asymmetry at the detector level of $(12 \pm 8)\%$. The first CDF measurement in 1.9 fb^{-1} [84] yielded $(24 \pm 14)\%$ at parton level. Both values were higher, though statistically consistent with the SM expectation. With the addition of more data, the uncertainties have been reduced, but the

measured asymmetries remain in excess of the SM expectation. The most recent measurement from DØ in 5.4 fb^{-1} finds an asymmetry, corrected for detector acceptance and resolution, of $(19.6 \pm 6.5)\%$ [85]. From CDF, the most recent measurement uses 9.4 fb^{-1}, and finds $(16.4 \pm 4.7)\%$ [86]. With additional data they report further evidence for an $M_{t\bar{t}}$-dependent asymmetry first reported in [87], with a larger asymmetry at large $M_{t\bar{t}}$ and an approximately linear dependence with $M_{t\bar{t}}$. DØ does not see any significant increase at large mass [85]. The new CDF measurement also includes a differential measurement of A_{FB} in bins of $|\Delta y|$ which also shows an approximately linear dependence with a positive slope. The SM prediction is also for an approximately linear dependence with a positive slope, but these studies show that the excess above the SM prediction occurs primarily at large values of these parameters. A further study of the dependence of A_{FB} on the p_T of the $t\overline{t}$ system indicates that the asymmetry is independent of the transverse momentum of the $t\overline{t}$ system.

At the LHC, where the dominant $t\overline{t}$ production mechanism is the charge-symmetric gluon-gluon fusion, the measurement is more difficult. For the sub-dominant $q\overline{q}$ production mechanism, the symmetric pp collision does not define a forward and backward direction. Instead, the charge asymmetry, A_C, is defined in terms of a positive versus a negative $t - \overline{t}$ rapidity difference

$$A_C = \frac{N(\Delta|y| > 0) - N(\Delta|y| < 0)}{N(\Delta|y| > 0) + N(\Delta|y| < 0)} \tag{3}$$

Both CMS and ATLAS have measured A_C in the LHC dataset. Using lepton+jets events in 4.7 fb^{-1} of data at $\sqrt{s} = 7$ TeV, ATLAS measures $A_C = (0.6 \pm 1.0)\%$ [88]. CMS, in 5.0(19.7) fb^{-1} of $\sqrt{s} = 7(8)$ TeV data uses lepton+jets events to measure $A_C = (0.4 \pm 1.5)\%$ ($A_C = (0.005 \pm 0.007(stat.) \pm 0.006(syst.))$) [89,90]. Both measurements are consistent with the SM expectation of $A_C = 1.23 \pm 0.05\%$ [81], although the uncertainties are still too large for a precision test. In their 7 and 8 TeV analyses, both, ATLAS and CMS, also provide differential measurements as a function of the $t\bar{t}$ mass, the transverse momentum p_T and the rapidity y.

Another avenue for measuring the forward-backward and charge asymmetries that has recently been exploited by the experiments is given by the measurement of the pseudorapidity distributions of the charged leptons resulting from $t\bar{t}$ decay. Although the expected asymmetry is smaller, this technique does not require the reconstruction of the top-quark direction. Single-lepton asymmetries are defined by $q \times \eta$, and dilepton asymmetries by the sign of $\Delta\eta$, where q and η are the charge and pseudorapidity of the lepton and $\Delta\eta = \eta_{\ell^+} - \eta_{\ell^-}$. DØ has recently measured the single-lepton asymmetry in 9.7 fb^{-1} of lepton+jets events, and finds a value of $(4.7 \pm 2.3^{+1.1}_{-1.4})\%$ [91], consistent with an expectation of $(3.8 \pm 0.6)\%$ [81]. A measurement by DØ using dilepton events in the same dataset [92] yields a dilepton asymmetry of $(12.3 \pm 5.4 \pm 1.5)$, less than two standard deviations away from the expectation of $(4.0 \pm 0.4)\%$ [81]. CDF, in 9.4 fb^{-1} of Tevatron data measures [93] $(9.4^{+3.2}_{-2.9})\%$. As in the DØ case, this is larger than the SM expectation, but less than two standard deviations away.

At the LHC, both ATLAS and CMS have now measured leptonic asymmetries. ATLAS, in 4.7 fb^{-1} of $\sqrt{s} = 7$ TeV data, has measured an asymmetry in dilepton events of $(2.3 \pm 1.2 \pm 0.8)\%$ [94]. CMS, in 5.0 fb^{-1} of $\sqrt{s} = 7$ TeV data, uses dilepton events to measure an asymmetry of $(1.0 \pm 1.5 \pm 0.6)\%$ [95]. Both of these are consistent, within their large uncertainties, with the SM expectation, derived by the experiments from the `MC@NLO` and `POWHEG` generators, respectively, of about 0.4%.

A model-independent comparison of the Tevatron and LHC results is made difficult by the differing $t\bar{t}$ production mechanisms at work at the two accelerators and by the symmetric nature of the pp collisions at the LHC. Given a particular model of BSM physics, a comparison can be obtained through the resulting asymmetry predicted by the model at the two machines, see Fig. 3.

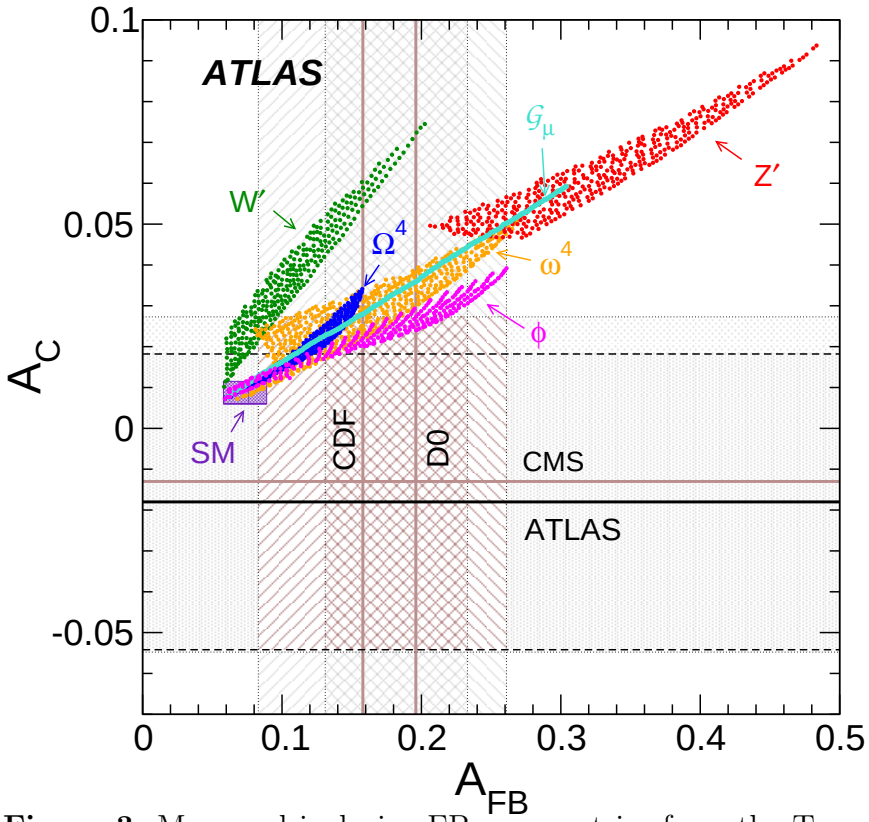

Figure 3: Measured inclusive FB asymmetries from the Tevatron and charge asymmetries from the LHC, compared to predictions from the SM as well as predictions incorporating various potential new physics contributions. The horizontal (vertical) bands and lines correspond to the ATLAS and CMS (CDF and DØ) measurements [96].

C.2 Top-Quark Properties

C.2.1 Top-Quark Mass Measurements: The most precisely studied property of the top quark is its mass. The top-quark mass has been measured in the lepton+jets, the dilepton, and the all-jets channel by all four Tevatron and LHC experiments. The latest and/or most precise results are summarized in Table 1. The lepton+jets channel still yields the most precise single measurements because of good signal to background (in particular after b-tagging) and the presence of only a single neutrino in the final state. The momentum of a single neutrino can be reconstructed (up to a quadratic ambiguity) via the missing E_T measurement and the constraint that the lepton and neutrino momenta reconstruct to the known W boson mass. In the

large data samples available at the LHC, measurements in the dilepton channel are only slightly less precise.

A large number of techniques have now been applied to measuring the top-quark mass. The original 'template method' [97], in which Monte Carlo templates of reconstructed mass distributions are fit to data, has evolved into a precision tool in the lepton+jets channel, where the systematic uncertainty due to the jet energy scale (JES) uncertainty is controlled by a simultaneous, *in situ*, fit to the $W \to jj$ hypothesis [98]. All the latest measurements in the lepton+jets and the all-jets channels use this technique one way or the other. In 4.7 fb^{-1} of data in the lepton+jets channel, ATLAS and CMS achieve a total uncertainty of 0.9% and 0.6%, with a statistical component of 0.44% [99] and 0.25% [100], respectively. The ATLAS measurement is in fact based on a 3-dimensional template fit, determining the top-quark mass, the global jet energy scale and a b-to-light jet energy scale factor. The measurement from CDF with 8.7 fb^{-1} [101] achieves a precision of 0.6% in the lepton+jets channel, while DØ achieves 0.9% in 3.6 fb^{-1} [102].

The template method is complemented by the 'matrix element' method. This method was first applied by the DØ Collaboration [103], and is similar to a technique originally suggested by Kondo *et al.* [104] and Dalitz and Goldstein [105]. In the matrix element method a probability for each event is calculated as a function of the top-quark mass, using a LO matrix element for the production and decay of $t\bar{t}$ pairs. The *in situ* calibration of dijet pairs to the $W \to jj$ hypothesis is now also used with the matrix element technique to constrain the jet energy scale uncertainty. The latest measurement with this technique is from DØ in the lepton+jets channel with 3.6 fb^{-1} yielding an uncertainty of about 0.9% [102].

CMS has measured the top-quark mass at LHC using an 'ideogram' method, first used by DØ [106], in which a constrained fit is performed and an event-by-event likelihood for signal or background is calculated taking into account all jet-parton assignments. In the lepton+jets channel at CMS, with an *in situ* fit of the JES using $W \to jj$, the measurement

has a precision of 1.07 GeV (0.6%) in 5 fb^{-1} [100], which is the most precise top-quark mass measurement to date.

In the dilepton channel, the signal to background is typically very good, but reconstruction of the mass is non-trivial because there are two neutrinos in the final state, yielding a kinematically unconstrained system. A variety of techniques has been developed to handle this. An analytic solution to the problem has been proposed [107], but this has not yet been used in the mass measurement. One of the two most precise measurements in the dilepton channel currently comes from using the invariant mass of the charged lepton and b-quark system ($M_{\ell b}$), which is sensitive to the top-quark mass and avoids the kinematic difficulties of the two-neutrino final state. In 4.7 fb^{-1} of data, ATLAS has measured the top-quark mass in the dilepton channel to a precision of 0.9% using a template fit to the $M_{\ell b}$ distribution [108]. The other dilepton-channel measurement of similar precision comes from 5.0 fb^{-1} of CMS data [109] using a so-called analytical matrix weighting technique (AMWT) in which each event is fit many times to a range of top-quark masses and each fit is assigned a weight, from the PDFs, given by the inferred kinematics of the initial state partons, and from the probability of the observed charged lepton energies for the top-quark mass in question.

Several other techniques can also yield precise measurements in the dilepton channel. In the neutrino weighting technique, similar to AMWT above, a weight is assigned by assuming a top-quark mass value and applying energy-momentum conservation to the top-quark decay, resulting in up to four possible pairs of solutions for the neutrino and anti-neutrino momenta. The missing E_T calculated in this way is then compared to the observed missing E_T to assign a weight [110]. Another measurement in the dilepton channel uses the Dalitz and Goldstein technique [111–113].

In the all-jets channel there is no ambiguity due to neutrino momenta, but the signal to background is significantly poorer due to the severe QCD multijets background. The emphasis therefore has been on background modeling, and reduction through event selection. The most recent measurement in the

all-jets channel, by CMS in 3.54 fb^{-1} [114], uses an ideogram method to extract the top-quark mass and achieves a precision of 0.8%. Here, the 1-dimensional fit for the top-mass with fixed jet energy scale is expected to be more precise than the 2-dimensional simultaneous fit for m_t and the jet energy scale. A recent measurement from ATLAS [115] uses the template method in the all-hadronic channel, also with an *in situ*, fit to the $W \to jj$ hypothesis, yielding a measurement with 2% precision in only 2.0 fb^{-1} of data. A measurement from CDF in 5.7 fb^{-1} uses a neural net to select events with a missing E_T plus jets signature [116]. A modified template method is used to extract the top-quark mass, including an *in situ* $W \to jj$ fit. A precision of 1% is achieved.

A dominant systematic uncertainty in these methods is the understanding of the jet energy scale, and so several techniques have been developed that have little sensitivity to the jet energy scale uncertainty. These include the measurement of the top-quark mass using the following techniques: Fitting of the lepton p_T spectrum of candidate events [117]; fitting of the transverse decay length of the b-jet (L_{xy}) [118]; fitting the invariant mass of a lepton from the W-decay and a muon from the semileptonic b decay [119].

Several measurements have now been made in which the top-quark mass is extracted from the measured cross section using the theoretical relationship between the mass and the production cross section, which allows the direct extraction of the $\overline{\rm MS}$ mass section [120].

Combined measurements from the Tevatron experiments and from the LHC experiments take into account the correlations between different measurements from a single experiment and between measurements from different experiments. The Tevatron average [3], using up to 8.7 fb^{-1} of data, now has a precision of 0.5%. The LHC combination, using up to 4.9 fb^{-1} of data, has a precision of just over 0.5% [121], where more work on systematic uncertainties is required. A Tevatron-LHC combination is not yet available.

The direct measurements of the top-quark mass, such as those shown in Table 1, are generally assumed to be measurements of the pole mass. Strictly speaking, the mass measured in these direct measurements is the mass used in the Monte Carlo generators. The relation between the Monte Carlo generator mass and the pole mass is uncertain at the level of 1 GeV [123], which is now comparable to the measurement uncertainty. A review of top-quark mass measurements can be found in reference [124].

Table 1: Measurements of top-quark mass from Tevatron and LHC. $\int \mathcal{L}\mathrm{dt}$ is given in fb^{-1}. The results shown are mostly preliminary (not yet submitted for publication as of September 2013); for a complete set of published results see the Listings. Statistical uncertainties are listed first, followed by systematic uncertainties.

m_t (GeV/c^2)	Source	$\int \mathcal{L}\mathrm{dt}$	Ref.	Channel
$174.94 \pm 1.14 \pm 0.96$	DØ Run II	3.6	[102]	ℓ+jets
$172.85 \pm 0.71 \pm 0.85$	CDF Run II	8.7	[101]	ℓ+jets
$173.93 \pm 1.64 \pm 0.87$	CDF Run II	8.7	[116]	Missing E_T+jets
$172.5 \pm 1.4 \pm 1.5$	CDF Run II	5.8	[122]	All jets
$172.31 \pm 0.75 \pm 1.35$	ATLAS	4.7	[99]	ℓ+jets
$173.09 \pm 0.64 \pm 1.50$	ATLAS	4.7	[108]	$\ell\ell$
$174.9 \pm 2.1 \pm 3.8$	ATLAS	2.04	[115]	All jets
$173.49 \pm 0.43 \pm 0.98$	CMS	5.0	[100]	ℓ+jets
$172.5 \pm 0.4 \pm 1.5$	CMS	5.0	[109]	$\ell\ell$
$173.49 \pm 0.69 \pm 1.21$	CMS	3.54	[114]	All jets
$173.20 \pm 0.51 \pm 0.71$ *	CDF,DØ (I+II)	$\leq$8.7	[3]	publ. or prelim. res.
$173.29 \pm 0.23 \pm 0.92$ *	ATLAS, CMS	$\leq$4.9	[121]	publ. or prelim. res.

*The Tevatron average is a combination of published Run I and preliminary or pub. Run-II meas., yielding a χ^2 of 8.5 for 11 deg. of freedom. The LHC average includes both published and preliminary results, yielding a χ^2 of 1.8 for 4 deg. of freedom.

With the discovery of a Higgs boson at the LHC with a mass of about 126 GeV [125,126], the precision measurement of the top-quark mass takes a central role in the question of the stability of the electroweak vacuum because top-quark radiative corrections tend to drive the Higgs quartic coupling, λ, negative, potentially leading to an unstable vacuum. A recent calculation at NNLO [127] leads to the conclusion of vacuum stability for a Higgs mass satisfying $M_H \geq 129.4 \pm 5.6$ GeV [128]. Given the uncertainty, a Higgs mass of 126 GeV satisfies the limit, but the central value of the Higgs and top-quark masses put the electroweak vacuum squarely in the metastable region. The uncertainty is dominated by the precision of the top-quark mass measurement and its interpretation as the pole mass. For more details, see the Higgs boson review in this volume.

As a test of the CPT-symmetry, the mass difference of top- and antitop-quarks $\Delta m_t = m_t - m_{\bar{t}}$, which is expected to be zero, can be measured. CDF measures the mass difference in 8.7 fb^{-1} of 1.96 TeV data in the lepton+jets channel using a template methode to find $\Delta m_t = -1.95 \pm 1.11(stat.) \pm 0.59(syst.)$ GeV/c^2 [129] while DØ uses 3.6 fb^{-1} of lepton+jets events and the matrix element method with at least one b-tag. They find $\Delta m_t = 0.8 \pm 1.8(stat.) \pm 0.5(syst.)$ GeV/c^2 [130]. In 4.7 fb^{-1} of 7 TeV data, ATLAS measures the mass difference in lepton+jets events with a double b-tag requirement and hence very low background to find $\Delta m_t = 0.67 \pm 0.61(stat.) \pm 0.41(syst.)$ GeV/c^2 [131]. CMS measures the top-quark mass difference in 5 fb^{-1} of 7 TeV data in the lepton+jets channel and finds $\Delta m_t = -0.44 \pm 0.46(stat.) \pm 0.27(syst.)$ GeV/c^2 [132]. They repeat this measurement with 18.9 fb^{-1} of 8 TeV data to find $\Delta m_t = -0.27 \pm 0.20(stat.) \pm 0.12(syst.)$ GeV/c^2 [133]. All measurements are consistent with the SM expectation.

C.2.2 Top-Quark Spin Correlations and Width: One of the unique features of the top quark is that it decays before its spin can be flipped by the strong interaction. Thus the top-quark polarization is directly observable via the angular distribution of its decay products. Hence, it is possible to define and measure observables sensitive to the top-quark spin

and its production mechanism. Although the top- and antitop-quarks produced by strong interactions in hadron collisions are essentially unpolarized, the spins of t and $\bar{t}$ are correlated. For QCD production at threshold, the $t\bar{t}$ system is produced in a $^3S_1$ state with parallel spins for $q\bar{q}$ annihilation or in a $^1S_0$ state with antiparallel spins for gluon-gluon fusion. Hence, the situations at the Tevatron and at the LHC are complementary. The direction of the top-quark spin is 100% correlated to the angular distributions of the down-type fermion (charged leptons or d-type quarks) in the decay. The joint angular distribution [134–136]

$$\frac{1}{\sigma}\frac{d^2\sigma}{d(\cos\theta_+)d(\cos\theta_-)} = \frac{1+\kappa\cdot\cos\theta_+\cdot\cos\theta_-}{4}, \qquad (4)$$

where θ_+ and θ_- are the angles of the daughters in the top-quark rest frame with respect to a particular spin quantization axis, is a very sensitive observable. The maximum value for κ, 0.782 at NLO at the Tevatron [137], is found in the off-diagonal basis [134], while at the LHC the value at NLO is 0.326 in the helicity basis [137]. The spin correlation could be modified by a new $t\bar{t}$ production mechanism such as through a Z' boson, Kaluza-Klein gluons, or a Higgs boson.

CDF used 5.1 fb^{-1} in the dilepton channel to measure the correlation coefficient in the beam axis [138]. The measurement was made using the expected distributions of $(\cos\theta_+, \cos\theta_-)$ and $(\cos\theta_b, \cos\theta_{\bar{b}})$ of the charged leptons or the b-quarks in the $t\bar{t}$ signal and background templates to calculate a likelihood of observed reconstructed distributions as a function of assumed κ. They determined the 68% confidence interval for the correlation coefficient κ as $-0.52 < \kappa < 0.61$ or $\kappa = 0.04 \pm 0.56$ assuming $m_t = 172.5$ GeV/c^2.

CDF also analyzed lepton+jets events in 5.3 fb^{-1} [139] assuming $m_t = 172.5$ GeV/c^2. They form three separate templates - the same-spin template, the opposite-spin template, and the background template for the 2-dimensional distributions in $\cos(\theta_l)\cos(\theta_d)$ vs. $\cos(\theta_l)\cos(\theta_b)$. The fit to the data in the helicity basis returns an opposite helicity fraction of $F_{OH} = 0.74 \pm 0.24(stat) \pm 0.11(syst)$. Converting this to the spin correlation coefficient yields $\kappa_{helicity} = 0.48 \pm 0.48(stat) \pm 0.22(syst)$.

In the beamline basis, they find an opposite spin fraction of $F_{OS} = 0.86 \pm 0.32(stat) \pm 0.13(syst)$ which can be converted into a correlation coefficient of $\kappa_{beam} = 0.72 \pm 0.64(stat) \pm 0.26(syst)$.

DØ performed a measurement of the ratio f of events with correlated t and $\bar{t}$ spins to the total number of $t\bar{t}$ events in 5.3 fb^{-1} in the lepton+jets channel using a matrix element technique [140]. From 729 events, they obtain $f_{meas} = 1.15^{+0.42}_{-0.43}$ (stat + syst) and can exclude values of $f < 0.420$ at the 95% C.L. In the dilepton channel [141], they also use a matrix element method and can exclude at the 97.7% C.L. the hypothesis that the spins of the t and $\bar{t}$ are uncorrelated. The combination [140] yields $f_{meas} = 0.85 \pm 0.29$ (stat + syst) and a $t\bar{t}$ production cross section which is in good agreement with the SM prediction and previous measurements. For an expected fraction of $f = 1$, they can exclude $f < 0.481$ at the 95% C.L. For the observed value of $f_{meas} = 0.85$, they can exclude $f < 0.344(0.052)$ at the 95(99.7)% C.L. The observed fraction f_{meas} translates to a measured asymmetry value of $A_{meas} = 0.66 \pm 0.23$ (stat + syst), where the spin correlation coefficient, A, is defined as

$$A = \frac{N(\uparrow\uparrow) + N(\downarrow\downarrow) - N(\uparrow\downarrow) - N(\downarrow\uparrow)}{N(\uparrow\uparrow) + N(\downarrow\downarrow) + N(\uparrow\downarrow) + N(\downarrow\uparrow),} \quad (5)$$

where the first arrow represents the direction of the top-quark spin along a chosen quantization axis, and the second arrow represents the same for the antitop-quark. They therefore obtain first evidence of SM spin correlation at 3.1 standard deviations.

Using 5.4 fb^{-1} of data, DØ measures the correlation in the dilepton channel also from the angles of the two leptons in the t and $\bar{t}$ rest frames, yielding a correlation strength $C = 0.10 \pm 0.45$ [142](C is equivalent to the opposite of κ in Eq. 4, in agreement with the NLO QCD prediction, but also in agreement with the no correlation hypothesis).

Spin correlations have now been conclusively measured at the LHC by both the ATLAS and CMS collaborations. In the dominant gluon fusion production mode for $t\bar{t}$ pairs at the LHC, the angular distribution between the two leptons in $t\bar{t}$ decays to dileptons is sensitive to the degree of spin correlation [143].

The ATLAS collaboration has performed a study of spin correlations in $t\bar{t}$ production at $\sqrt{s} = 7$ TeV using 2.1 fb^{-1} of data. Candidate events are selected in the dilepton topology with large missing transverse energy and at least two jets. The difference in azimuthal angle between the two charged leptons is compared to the expected distributions in the Standard Model, and to the case where the top quarks are produced with uncorrelated spin. Using the helicity basis as the quantization axis, the strength of the spin correlation between the top- and antitop-quark is measured to be $A_{helicity} = 0.40^{+0.09}_{-0.08}$ [144], which is in agreement with the NLO prediction of about 0.31 [145]. The hypothesis of no spin correlations is excluded at 5.1 standard deviations. An update of this analysis with 4.6 fb^{-1} yields results for four different variables, which have sensitivity to different properties of the production mechanism. The results can be translated to $A_{helicity} = 0.37 \pm 0.06(stat. + syst.)$ [146].

A similar analysis at CMS using dilepton events in 5.0 fb^{-1} of pp collisions at $\sqrt{s} = 7$ TeV. The angular distribution between the two leptons is fit to extract $A_{helicity} = 0.24 \pm 0.02 \pm 0.08$ [147].

Observation of top-quark spin correlations requires a top-quark lifetime less than the spin decorrelation timescale [148]. The top-quark width, inversely proportional to its lifetime, is expected to be of order 1 GeV/c^2 (Eq. 1). The sensitivity of current experiments does not approach this level in direct measurements. Nevertheless, several measurements have been made.

CDF presents a direct measurement of the top-quark width in the lepton+jets decay channel of $t\bar{t}$ events from a data sample corresponding to 8.7 fb^{-1} of integrated luminosity. The top-quark mass and the mass of the hadronically decaying W boson that comes from the top-quark decay are reconstructed for each event and compared with templates of different top-quark widths (Γ_t) and deviations from nominal jet energy scale (ΔJES) to perform a simultaneous fit for both parameters, where ΔJES is used for the $in\ situ$ calibration of the jet energy scale. By applying a Feldman-Cousins approach, they establish

an upper limit at 95% C.L. of $\Gamma_t < 6.38$ GeV and a two-sided 68% C.L. interval of 1.10 GeV $< \Gamma_t <$ 4.05 GeV, corresponding to a lifetime interval of $1.6 \times 10^{-15} < \tau_{top} < 6.0 \times 10^{-25}$ [149], consistent with the SM prediction. For comparison, a typical hadronization timescale is an order of magnitude larger than these limits.

DØ extracts the total width of the top-quark from the partial decay width $\Gamma(t \to Wb)$ and the branching fraction $B(t \to Wb)$. $\Gamma(t \to Wb)$ is obtained from the measured t-channel cross section for single top-quark production in 5.4 fb^{-1}, and $B(t \to Wb)$ is extracted from a measurement of the ratio $R = B(t \to Wb)/B(t \to Wq)$ in $t\bar{t}$ events in lepton+jets channels with 0, 1 and 2 b-tags. Assuming $B(t \to Wq) = 1$, where q includes any kinematically accessible quark, the result is: $\Gamma_t = 2.00^{+0.47}_{-0.43}$ GeV which translates to a top-quark lifetime of $\tau_t = (3.29^{+0.90}_{-0.63}) \times 10^{-25}$ s. Assuming a high mass fourth generation b' quark and unitarity of the four-generation quark-mixing matrix, they set the first upper limit on $|V_{tb'}| < 0.59$ at 95% C.L. [150].

C.2.3 W-Boson Helicity in Top-Quark Decay: The Standard Model dictates that the top quark has the same vector-minus-axial-vector $(V - A)$ charged-current weak interactions $\left(-i\frac{g}{\sqrt{2}}V_{tb}\gamma^{\mu}\frac{1}{2}(1-\gamma_5)\right)$ as all the other fermions. In the SM, the fraction of top-quark decays to longitudinally polarized W bosons is similar to its Yukawa coupling and hence enhanced with respect to the weak coupling. It is expected to be [151] $\mathcal{F}_0^{\rm SM} \approx x/(1+x)$, $x = m_t^2/2M_W^2$ ($\mathcal{F}_0^{\rm SM} \sim 70\%$ for $m_t = 175$ GeV/c^2). Fractions of left-handed, right-handed, or longitudinal W bosons are denoted as $\mathcal{F}_-$, $\mathcal{F}_+$, and $\mathcal{F}_0$ respectively. In the SM, $\mathcal{F}_-$ is expected to be $\approx 30\%$ and $\mathcal{F}_+ \approx 0\%$. Predictions for the W polarization fractions at NNLO in QCD are available [152].

The Tevatron and the LHC experiments use various techniques to measure the helicity of the W boson in top-quark decays, in both the lepton+jets and in dilepton channels in $t\bar{t}$ production.

The first method uses a kinematic fit, similar to that used in the lepton+jets mass analyses, but with the top-quark mass constrained to a fixed value, to improve the reconstruction of final-state observables, and render the under-constrained dilepton channel solvable. Alternatively, in the dilepton channel θ^* can also be obtained through an algebraic solution of the kinematics. The distribution of the helicity angle ($\cos\theta^*$) between the lepton and the b quark in the W rest frame provides the most direct measure of the W helicity. In a simplified version of this approach, the $\cos\theta^*$ distribution is reduced to a forward-backward asymmetry.

The second method (p_T^ℓ) uses the different lepton p_T spectra from longitudinally or transversely polarized W-decays to determine the relative contributions.

A third method uses the invariant mass of the lepton and the b-quark in top-quark decays ($M^2_{\ell b}$) as an observable, which is directly related to $\cos\theta^*$.

At the LHC, top-quark pairs in the dilepton channels are reconstructed by solving a set of six independent kinematic equations on the missing transverse energy in x- and in y-direction, two W-masses, and the two top/antitop-quark masses. In addition, the two jets with the largest p_T in the event are interpreted as b-jets. The pairing of the jets to the charged leptons is based on the minimization of the sum of invariant masses m_{min}. Simulations show that this criterion gives the correct pairing in 68% of the events.

Finally, the Matrix Element method (ME) has also been used, in which a likelihood is formed from a product of event probabilities calculated from the ME for a given set of measured kinematic variables and assumed W-helicity fractions. The results of recent CDF, DØ, ATLAS, and CMS analyses are summarized in Table 2.

The datasets are now large enough to allow for a simultaneous fit of $\mathcal{F}_0$, $\mathcal{F}_-$ and $\mathcal{F}_+$, which we denote by '3-param' or $\mathcal{F}_0$ and $\mathcal{F}_+$, which we denote by '2-param' in the table. Results with either $\mathcal{F}_0$ or $\mathcal{F}_+$ fixed at its SM value are denoted '1-param'. For the simultaneous fits, the correlation coefficient

between the two values is about −0.8. A complete set of published results can be found in the Listings. All results are in agreement with the SM expectation.

CDF and DØ combined their results based on 2.7 − 5.4 fb^{-1} using the BLUE method [153] for a top-quark mass of 172.5 GeV/c^2. ATLAS presents results from 1.04 fb^{-1} of $\sqrt{s}$ = 7 TeV data using a template method for the $\cos\theta^*$ distribution and angular asymmetries from the unfolded $\cos\theta^*$ distribution in the lepton+jets and the dilepton channel [155]. CMS performs a similar measurement based on template fits to the $\cos\theta^*$ distribution with 5.0 fb^{-1} of 7 TeV data in the lepton+jets final state [156]. As the polarization of the W bosons in top-quark decays is sensitive to the $W-t-b$ vertex Lorentz structure and anomalous couplings, both experiments also derive limits on anomalous contributions to the $W-t-b$ couplings. Recently, both experiments also combined their results from 7 TeV data to obtain values on the helicity fractions as well as limits on anomalous couplings [157]. Very recently, CMS came out with a measurement of the W-helicity fractions in 19.6 fb^{-1} of muon+jets events recorded at 8 TeV [158]. Also, a first measurement of the W-boson helicity in top-quark decays was made in electroweak single top production [159], yielding consistent results.

C.2.4 Top-Quark Electric Charge: The top quark is the only quark whose electric charge has not been measured through production at threshold in e^+e^- collisions. Furthermore, it is the only quark whose electromagnetic coupling has not been observed and studied until recently. Since the CDF and DØ analyses on top-quark production did not associate the b, $\bar{b}$, and $W^\pm$ uniquely to the top or antitop, decays such as $t \to W^+\bar{b}, \bar{t} \to W^-b$ were not excluded. A charge 4/3 quark of this kind is consistent with current electroweak precision data. The $Z \to \ell^+\ell^-$ and $Z \to b\bar{b}$ data, in particular the discrepancy between A_{LR} from SLC at SLAC and $A_{FB}^{0,b}$ of b-quarks and $A_{FB}^{0,\ell}$ of leptons from LEP at CERN, can be fitted with a top quark of mass $m_t = 270$ GeV/c^2, provided that the right-handed b quark mixes with the isospin +1/2 component of an exotic doublet of charge −1/3 and −4/3 quarks, $(Q_1, Q_4)_R$ [160,161].

Table 2: Measurement and 95% C.L. upper limits of the W helicity in top-quark decays. The table includes both preliminary, as of September 2013, and published results. A full set of published results is given in the Listings.

W Helicity	Source	$\int \mathcal{L}$dt (fb^{-1})	Ref.	Method
$\mathcal{F}_0 = 0.722 \pm 0.081$	CDF+DØ Run II	2.7-5.4	[153]	$\cos\theta^*$ 2-param
$\mathcal{F}_0 = 0.682 \pm 0.057$	CDF+DØ Run II	2.7-5.4	[153]	$\cos\theta^*$ 1-param
$\mathcal{F}_0 = 0.726 \pm 0.094$	CDF Run II	8.7	[154]	ME 2-param
$\mathcal{F}_0 = 0.67 \pm 0.07$	ATLAS	1.0	[155]	$\cos\theta^*$ 3-param
$\mathcal{F}_0 = 0.682 \pm 0.045$	CMS	5.0	[156]	$\cos\theta^*$ 3-param
$\mathcal{F}_0 = 0.626 \pm 0.059$	ATLAS+CMS (7 TeV)	2.2	[157]	$\cos\theta^*$ 3-param
$\mathcal{F}_0 = 0.659 \pm 0.027$	CMS (8 TeV)	19.6	[158]	$\cos\theta^*$ 3-param
$\mathcal{F}_+ = -0.033 \pm 0.046$	CDF+DØ Run II	2.7-5.4	[153]	$\cos\theta^*$ 2-param
$\mathcal{F}_+ = -0.015 \pm 0.035$	CDF+DØ Run II	2.7-5.4	[153]	$\cos\theta^*$ 1-param
$\mathcal{F}_+ = -0.045 \pm 0.073$	CDF Run II	8.7	[154]	ME 2-param
$\mathcal{F}_+ = 0.01 \pm 0.05$	ATLAS	1.0	[155]	$\cos\theta^*$ 3-param
$\mathcal{F}_+ = 0.008 \pm 0.018$	CMS	5.0	[156]	$\cos\theta^*$ 3-param
$\mathcal{F}_+ = 0.015 \pm 0.034$	ATLAS+CMS (7 TeV)	2.2	[157]	$\cos\theta^*$ 3-param
$\mathcal{F}_+ = 0.009 \pm 0.021$	CMS (8 TeV)	19.6	[158]	$\cos\theta^*$ 3-param

DØ studies the top-quark charge in double-tagged lepton+jets events, CDF does it in single tagged lepton+jets and dilepton events. Assuming the top- and antitop-quarks have equal but opposite electric charge, then reconstructing the charge of the b-quark through jet charge discrimination techniques, the $|Q_{top}| = 4/3$ and $|Q_{top}| = 2/3$ scenarios can be differentiated. For the exotic model of Chang *et al.* [161] with a top-quark charge $|Q_{top}| = 4/3$, DØ excludes the exotic model at 91.2% C.L.% [162] using 370 pb^{-1}, while CDF excludes the model at 99% C.L. [163] in 5.6 fb^{-1}. Both results indicate that the observed particle is indeed consistent with being a SM $|Q_{top}| = 2/3$ quark.

In 2.05 fb^{-1} at $\sqrt{s} = 7$ TeV, ATLAS performed a similar analysis, reconstructing the b-quark charge either via a jet-charge technique or via the lepton charge in soft muon decays in combination with a kinematic likelihood fit. They measure the top-quark charge to be $0.64 \pm 0.02(stat.) \pm 0.08(syst.)e$ from the charges of the top-quark decay products in single lepton $t\bar{t}$ events, and hence exclude the exotic scenario with charge $-4/3$ at more than 8σ [164].

In 4.6 fb^{-1} at $\sqrt{s} = 7$ TeV, CMS discriminates between the Standard Model and the exotic top-quark charge scenario in the muon+jets final states in $t\bar{t}$ events. They exploit the charge correlation between high-p_t muons from W-boson decays and soft muons from B-hadron decays in b-jets. Using an asymmetry technique, where $A = -1$ represent the exotic $q = -4/3$ scenario and $A = +1$ the Standard Model $q = +2/3$ scenario, they find $A_{meas} = 0.97 \pm 0.12(stat.) \pm 0.31(sys.)$, which agrees with the Standard Model expectation and excludes the exotics scenario at 99.9% C.L. [165].

The electromagnetic or the weak coupling of the top quark can be probed directly by investigating $t\bar{t}$ events with an additional gauge boson, like $t\bar{t}\gamma$ and $t\bar{t}Z$ events.

CDF performs a search for events containing a lepton, a photon, significant missing transverse momentum, and a jet identified as containing a b-quark and at least three jets and large total transverse energy in 6.0 fb^{-1}. They reported evidence for the observation of $t\bar{t}\gamma$ production with a cross section $\sigma_{t\bar{t}\gamma} = 0.18 \pm 0.08$ pb and a ratio of $\sigma_{t\bar{t}\gamma}/\sigma_{t\bar{t}} = 0.024 \pm 0.009$ [166].

ATLAS performed a first measurement of the $t\bar{t}\gamma$ cross section in pp collisions at $\sqrt{s} = 7$ TeV using 1.04 fb^{-1} of data. Events are selected that contain a large transverse momentum electron or muon and a large transverse momentum photon, yielding 52 and 70 events in the electron and muon samples, respectively. The resulting cross section times branching ratio into the single lepton and dilepton channels for $t\bar{t}\gamma$ production with a photon with transverse momentum above 8 GeV is $\sigma(t\bar{t}\gamma) = 2.0 \pm 0.5(stat.) \pm 0.7(syst.) \pm 0.1(lumi.)$ pb [167], which is consistent with theoretical calculations. A real test, however,

of the vector and axial vector couplings in $t\bar{t}\gamma$ events or searches for possible tensor couplings of top-quarks to photons will only be feasible with an integrated luminosity of several hundred fb^{-1} in the future.

CMS also performed measurements of the $t\bar{t}W$ and $t\bar{t}Z$ production cross section at $\sqrt{s} = 7$ TeV with 5 fb^{-1}, yielding results at about 3 standard deviations significance [168]. ATLAS performed a similar analysis with 4.7 fb^{-1} in the three-lepton channel and set an upper limit of 0.71 pb at 95% C.L. [169]. Also here, more data is expected to yield an observation.

C.3 Searches for Beyond the Standard Model Physics

The top quark plays a special role in the SM. Being the only quark with a coupling to the Higgs boson of order one, it provides the most important contributions to the quadratic radiative corrections to the Higgs mass raising the question of the naturalness of the SM. It is therefore very common for models where the naturalness problem is addressed to have new physics associated with the top quark. In SUSY, for instance, naturalness predicts the scalar top partners to be the lightest among the squarks and to be accessible at the LHC energies (see the review "Supersymmetry: Theory"). In models where the Higgs is a pseudo-Goldstone boson, such as Little Higgs models, naturalness predicts the existence of partners of the top quarks with the same spin and color, but with different electroweak couplings, the so-called vectorial t'. Stops and t''s are expected to have sizable branching ratios to top quarks. Another intriguing prediction of SUSY models with universal couplings at the unification scale is that for a top-quark mass close to the measured value, the running of the Yukawa coupling down to 1 TeV naturally leads to the radiative breaking of the electroweak symmetry [170]. In fact, the top quark plays a role in the dynamics of electroweak symmetry breaking in many models. One example is topcolor [171], where a large top-quark mass can be generated through the formation of a dynamic $t\bar{t}$ condensate, X, which is formed by a new strong gauge force coupling preferentially to the third generation. Another example is topcolor-assisted technicolor [172], predicting the existence of a heavy Z' boson that couples preferentially to the

third generation of quarks. If light enough such a state might be directly accessible at the present hadron collider energies, or if too heavy, lead to four-top interactions possibly visible in the production cross section for $t\bar{t}t\bar{t}$.

Current strategies to search for new physics in top-quark events at hadron colliders are either tailored to the discovery of specific models or model independent. They can be broadly divided in two classes. In the first class new resonant states are looked for through decay processes involving the top quarks. Current searches for bosonic resonances in $t\bar{t}$ final states, or for direct stop and t' production, or for a charged Higgs in $H^+ \to t\bar{b}$ fall in the category. On the other hand, if new states are too heavy to be directly produced, they might still give rise to deviations from the SM predictions for the strength and Lorentz form of the top-quark couplings to other SM particles. Accurate predictions and measurements are therefore needed and the results be efficiently systematized in the framework of an effective field theory [173,174]. The on-going efforts to constrain the $W - t - b$ coupling and to search for flavor-changing neutral currents involving the top quark fall in this second category.

C.3.1 New Physics in Top-Quark Production: Theoretical [175–177] and experimental efforts have been devoted to the searches for new physics in $t\bar{t}$ resonances.

At the Tevatron, both the CDF and DØ collaborations have searched for resonant production of $t\bar{t}$ pairs in the lepton+jets channel [182,183]. In both analyses, the data indicate no evidence of resonant production of $t\bar{t}$ pairs. They place upper limits on the production cross section times branching fraction to $t\bar{t}$ in comparison to the prediction for a narrow ($\Gamma_{Z'} = 0.012 M_{Z'}$) leptophobic topcolor Z' boson. Within this model, they exclude Z' bosons with masses below 915 (CDF-full data set) and 835 (DØ, 5 fb^{-1}) GeV/c^2 at the 95% C.L. These limits turn out to be independent of couplings of the $t\bar{t}$ resonance (pure vector, pure axial-vector, or SM-like Z'). A similar analysis has been performed by CDF in the all-jets channel using 2.8 fb^{-1} of data [184].

At the LHC, both the CMS and ATLAS collaborations have searched for resonant production of $t\bar{t}$ pairs, employing different techniques and final-state signatures (all-jets, lepton+jets, dilepton) at $\sqrt{s} = 7$ and 8 TeV. In the low mass range, from the $t\bar{t}$ threshold to about one TeV, standard techniques based on the reconstruction of each of the decay objects (lepton, jets and b-jets, missing E_T) are used to identify the top quarks, while at higher invariant mass, the top quarks are boosted and the decay products more collimated and can appear as large-radius jets with substructure. Dedicated reconstruction techniques have been developed in recent years for boosted top quarks [185] that are currently employed at the LHC. Most of the analyses are model-independent (i.e., no assumption on the quantum numbers of the resonance is made) yet they assume a small width and no signal-background interference.

Using dilepton and lepton+jets signatures in a data set corresponding to an integrated luminosity of 5.0 fb^{-1}, the CMS collaboration finds no significant deviations from the SM background. In the dilepton analysis, upper limits are presented for the production cross section times branching fraction of top quark-antiquark resonances for masses from 750 to 3000 GeV/c^2. In particular, the existence of a leptophobic topcolor particle Z' is excluded at the 95% confidence level for resonance masses $M_{Z'} < 1.3$ (1.9) TeV/c^2 for $\Gamma_{Z'} = 0.012(0.1)M_{Z'}$ [186]. Using a lepton+jets sample, results are obtained from the combination of two dedicated searches optimized for boosted production and production at threshold. In this case, topcolor Z' bosons with narrow (wide) width are excluded at 95% confidence level for masses below 1.49 (2.04) TeV/c^2 and an upper limit of 0.3 (1.3) pb or lower is set on the production cross section times branching fraction for resonance masses above 1 TeV/c^2. Kaluza-Klein excitations of a gluon with masses below 1.82 TeV/c^2 (at 95% confidence level) in the Randall-Sundrum model are also excluded, and an upper limit of 0.7 pb or lower is set on the production cross section times branching fraction for resonance masses above 1 TeV/c^2 [187]. In 19.7 fb^{-1} of 8 TeV data, CMS recently updated their measurement in the lepton+jets and the all-jets channel to obtain an

exclusion of $M_{Z'} < 2.1(2.7)$ TeV/c^2 for $\Gamma_{Z'} = 0.013(0.1)M_{Z'}$ and gluon masses below 2.5 TeV/c^2 in Randall-Sundrum models at 95% C.L. [188].

The ATLAS collaboration has performed a search for resonant $t\bar{t}$ production in the lepton+jets channel using 4.7 fb^{-1} (14 fb^{-1}) of proton-proton (pp) collision data collected at a center-of-mass energy $\sqrt{s} = 7(8)$ TeV [189,190]. The $t\bar{t}$ system is reconstructed using both small-radius and large-radius jets, the latter being supplemented by a jet substructure analysis. A search for local excesses in the number of data events compared to the Standard Model expectation in the $t\bar{t}$ invariant mass spectrum is performed. No evidence for a $t\bar{t}$ resonance is found and 95% confidence-level limits on the production rate are determined for massive states predicted in two benchmark models. The most stringent limits come from the sample collected at 8 TeV. The upper limits on the cross section times branching ratio of a narrow Z' boson decaying to top-quark pairs range from 5.3 pb for a resonance mass of 0.5 TeV/c^2 to 0.08 pb for a mass of 3 TeV/c^2. A narrow leptophobic topcolor Z' boson with a mass below 1.8 TeV/c^2 is excluded. Upper limits are set on the cross section times branching ratio for a broad color-octet resonance with $\Gamma/m = 15.3\%$ decaying to $t\bar{t}$. These range from 9.6 pb for a mass of 0.5 TeV/c^2 to 0.152 pb for a mass of 2.5 TeV/c^2. A Kaluza-Klein excitation of the gluon in a Randall-Sundrum model (a slightly different model is used compared to CMS) is excluded for masses below 2.0 TeV/c^2.

ATLAS has also conducted a search in the all-jet final state at 7 TeV corresponding to an integrated luminosity of 4.7 fb^{-1} [191]. The $t\bar{t}$ events are reconstructed by selecting two top quarks in their fully hadronic decay modes which are reconstructed using the Cambridge/Aachen jet finder algorithm with a radius parameter of 1.5. The substructure of the jets is analysed using the HEPTopTagger algorithm [192] to separate top-quark jets from those originating from gluons and lighter quark jets. The invariant mass spectrum of the data is compared to the SM prediction, and no evidence for resonant production of top-quark pairs is found. The data are used to set upper limits on the cross section times branching ratio for resonant $t\bar{t}$

production in two models at 95% confidence level. Leptophobic Z' bosons with masses between 700 and 1000 GeV/c^2 as well as $1280 - 1320$ GeV/c^2 and Kaluza-Klein-Gluons with masses between 700 and 1620 GeV/c^2 are excluded at the 95% confidence level.

Heavy charged bosons, such as W' or H^+, can also be searched for in $t\bar{b}$ final states (for more information see the review "W'-boson searches" and "Higgs Bosons: theory and searches"). Other resonances are searched for in final states such as tZ, tj, tH, tW, bW.

For instance, ATLAS has performed a search for t-jet resonances in the lepton+jets channel of $t\bar{t}+$ jets events in 4.7 fb^{-1} at $\sqrt{s} = 7$ TeV [193]. A heavy new particle, assumed to be produced singly in association with a $t(\bar{t})$ quark, decays to a $t(\bar{t})$ quark and a light flavor quark, leading to a color singlet (triplet) resonance in the $t(\bar{t})$+jet system. The full 2011 ATLAS pp collision dataset from the LHC (4.7 fb^{-1}) is used to select $t\bar{t}$ events. The data are consistent with the SM expectation and a new particle with mass below 350 (430) GeV/c^2 for W (color triplet) models is excluded with a 95% confidence level, assuming unit right-handed coupling. ATLAS has conducted a search for the pair production of a new charge +2/3 quark (T) decaying via $T \to Zt$ in a dataset corresponding to 14.3 fb^{-1} luminosity at $\sqrt{s} = 8$ TeV [194]. Selected events contain a high transverse momentum Z-boson candidate reconstructed from a pair of oppositely charged electrons or muons. Additionally, the presence of at least two jets possessing properties consistent with the decay of a b-hadron is required, as well as large total transverse momentum of all central jets in the event. No significant excess of events above the SM expectation is observed, and upper limits are derived for vector-like quarks of various masses in a two-dimensional plane of branching ratios. Under branching ratio assumptions corresponding to a weak-isospin singlet scenario, a T quark with mass lower than 585 GeV/c^2 is excluded at the 95% confidence level. Under branching ratio assumptions corresponding to a particular weak-isospin doublet scenario, a T quark with mass lower than 680 GeV/c^2 is excluded at the 95% confidence level.

A complementary search [195] in the lepton+jets final state of the same dataset, characterized by an isolated electron or muon with moderately high transverse momentum, significant missing transverse momentum, and at least six jets is performed to look for $T \to Wb, Ht$ decays. The search exploits the high total transverse momenta of all final state objects and the high multiplicity of b-jets characteristic of signal events with at least one Higgs boson decaying into $b\bar{b}$, to discriminate against the dominant background from top-quark pair production. No significant excess of events above the SM expectation is observed, and upper limits are derived for vector-like quarks of various masses in the two-dimensional plane of $B(T \to Wb)$ versus $B(T \to Ht)$, where H is the Standard Model Higgs boson, assumed to have a mass of 125 GeV/c^2. Under the branching ratio assumptions corresponding to a weak-isospin doublet (singlet) scenario, a T quark with mass lower than 790 (640) GeV/c^2 is excluded at the 95% C.L.

Finally, a more general search is performed in the same data set [196], looking for exotic processes that result in final states containing jets including at least one b-jet, sizable missing transverse momentum, and a pair of leptons with the same electric charge. In addition to the new physics signal discussed above, this study provides limits on four top-quark production and production of two positively-charged top quarks. No significant excess of events over the background expectation is observed. This observation is interpreted as constraining the signal hypotheses, and it is found at 95% C.L. level that: the lower bound on the fourth generation B quark mass, assuming 100% branching fraction to Wt, is 0.72 TeV/c^2; the mass of a vector-like B (T) quark, assuming branching ratios to W, Z, and H decay modes consistent with the B or T being a singlet, is larger than 0.59 (0.54) TeV/c^2; the four top production cross section must be less than 85 fb in the SM and less than 59 fb for production via a contact interaction; the mass of a sgluon must be greater than 0.80 TeV/c^2; in the context of models with two universal extra dimensions the inverse size of the extra dimensions must be larger 0.90 TeV/c^2; and the cross section

for production of two positively-charged top quarks must be smaller than 210 fb.

In many models top-quark partners preferably decay to top quarks and weakly interacting neutral stable particles that are not detected. An observable especially sensitive to new physics effects in $t\bar{t}$ production is therefore the missing momentum. CMS has presented a differential cross section measurement of top-quark pair production with missing transverse energy using 5.1 fb^{-1} of data collected at 7 TeV [197]. The analysis selects events in the lepton+jets final state and the differential cross section is measured in bins of missing transverse energy. Recently, CMS has updated their analysis with 20 fb^{-1} at 8 TeV [49]. The results are consistent with the predictions of the SM. An analogous search, but more targeted to discover new physics in $t\bar{t}$ events with large missing transverse momentum in proton-proton collisions at a center-of-mass energy of 7 TeV in 1.04 fb^{-1} of data has been performed by ATLAS [198]. The search is carried out in the lepton+jets channel. The results are interpreted in terms of a model where new top-quark partners are pair-produced and each decay to an on-shell top (or antitop) quark and a long-lived undetected neutral particle. The data are found to be consistent with SM expectations. A limit at 95% C.L. is set excluding a cross-section times branching ratio of 1.1 pb for a top-partner mass of 420 GeV/c^2 and a neutral particle mass less than 10 GeV/c^2. In a model of exotic fourth generation quarks, top-partner masses are excluded up to 420 GeV/c^2 and neutral particle masses up to 140 GeV/c^2.

Flavor-changing-neutral-currents (FCNC) are hugely suppressed in the SM, and non zero only due to the large mass hierarchy between the top quark and the other quarks. Several observables are accessible at colliders to test and constrain such couplings.

CMS has performed a study of top-quark couplings through the search for a single top quark produced in association with a Z boson in 5 fb^{-1} integrated luminosity at 7 TeV [199]. The event selection requires the presence of three isolated leptons, electrons or muons, and of at least one jet. The upper limits on effective coupling strength can be translated

to the 95% upper limits on the corresponding branching ratios $B(t \to gu) \leq 0.56\%$, $B(t \to gc) \leq 7.1\%$, $B(t \to Zu) \leq 0.51\%$, $B(t \to Zc) \leq 11\%$.

ATLAS has presented results on the search for single top-quark production via FCNC's in strong interactions using data collected at $\sqrt{s}$=8 TeV and corresponding to an integrated luminosity of 14.2 fb^{-1}. Flavor-changing-neutral-current events are searched for in which a light quark (u or c) interacts with a gluon to produce a single top quark, either with or without the associated production of another light quark or gluon. Candidate events of top quarks decaying into leptons and jets are selected and classified into signal- and background-like events using a neural network. The observed 95% C.L. $B(t \to ug) < 3.1 \cdot 10^{-5}$ and $B(t \to cg) < 1.6 \cdot 10^{-4}$ [200]. This result supersedes the corresponding 7 TeV analysis in 2 fb^{-1} [201].

Constraints on FCNC couplings of the top quark can also be obtained from searches for anomalous single top-quark production in e^+e^- collisions, via the process $e^+e^- \to \gamma, Z^* \to t\overline{q}$ and its charge-conjugate ($q = u, c$), or in $e^{\pm}p$ collisions, via the process $e^{\pm}u \to e^{\pm}t$. For a leptonic W decay, the topology is at least a high-p_T lepton, a high-p_T jet and missing E_T, while for a hadronic W-decay, the topology is three high-p_T jets. Limits on the cross section for this reaction have been obtained by the LEP collaborations [202] in e^+e^- collisions, and by H1 [203] and ZEUS [204] in $e^{\pm}p$ collisions. When interpreted in terms of branching ratios in top decay [205,206], the LEP limits lead to typical 95% C.L. upper bounds of $B(t \to qZ) < 0.137$. Assuming no coupling to the Z boson, the 95% C.L. limits on the anomalous FCNC coupling $\kappa_\gamma < 0.13$ and < 0.27 by ZEUS and H1, respectively, are stronger than the CDF limit of $\kappa_\gamma < 0.42$, and improve over LEP sensitivity in that domain. The H1 limit is slightly weaker than the ZEUS limit due to an observed excess of five-candidate events over an expected background of 3.2 ± 0.4. If this excess is attributed to FCNC top-quark production, this leads to a total cross section of $\sigma(ep \to e + t + X, \sqrt{s} = 319 \text{ GeV}) < 0.25$ pb [203,207].

C.3.2 New Physics in Top-Quark decays: The large sample of top quarks produced at the Tevatron and the LHC allows to measure or set stringent limits on the branching ratios of rare top-quark decays. For example, the existence of a light H^+ can be constrained by looking for $t \to H^+ b$ decay, in particular with tau-leptons in the final state (for more information see the review "Higgs Bosons: theory and searches").

A first class of searches for new physics focuses on the strcuture of the $W-t-b$ vertex. Using up to 2.7 fb^{-1} of data, DØ has measured the Wtb coupling form factors by combining information from the W-boson helicity in top-quark decays in $t\bar{t}$ events and single top-quark production, allowing to place limits on the left-handed and right-handed vector and tensor couplings [225–227].

More recently, ATLAS has published the results of a search for CP violation in the decay of single top quarks produced in the t-channel where the top quarks are predicted to be highly polarized, using the lepton+jets final state [228]. The data analyzed are from pp collisions at $\sqrt{s} = 7$ TeV and correspond to an integrated luminosity of 4.7 fb^{-1}. In the Standard Model, the couplings at the Wtb vertex are left-handed, right-handed couplings being absent. A forward-backward asymmetry with respect to the normal to the plane defined by the W-momentum and the top-quark polarization has been used to probe the complex phase of a possibly non-zero value of the right-handed coupling, signaling a source of CP-violation beyond the SM. The measured value of the asymmetry is $0.031 \pm 0.065(stat.)^{+0.029}_{-0.031}(syst.)$ in good agreement with the Standard Model.

A second class of searches focuses on FCNC's in the top-quark decays.

Both, CDF and DØ, have provided the first limits for FCNC's in Run I and II. The most recent results from CDF give $B(t \to qZ) < 3.7\%$ and $B(t \to q\gamma) < 3.2\%$ at the 95% C.L. [229] while DØ [230,231] sets $B(t \to qZ)(q = u, c$ quarks $) < 3.2\%)$ at 95% C.L., $B(t \to gu) < 2.0 \cdot 10^{-4}$, and $B(t \to gc) < 3.9 \cdot 10^{-3}$ at the 95% C.L.

At the LHC, CMS has used a sample at a center-of-mass energy of 8 TeV corresponding to 19.7 fb^{-1} of integrated luminosity to perform a search for flavor changing neutral current top-quark decay $t \to Zq$. Events with a topology compatible with the decay chain $t\bar{t} \to Wb + Zq \to \ell\nu\ b + \ell\ell q$ are searched for. There is no excess seen in the observed number of events relative to the SM prediction; thus no evidence for flavor changing neutral current in top-quark decays is found. A combination with a previous search at 7 TeV excludes a $t \to Zq$ branching fraction greater than 0.05% at the 95% confidence level [232].

The ATLAS collaboration has also searched for FCNC processes in 2.1 fb^{-1} of $t\bar{t}$ events with one top quark decaying through FCNC ($t \to qZ$) and the other through the SM dominant mode ($t \to bW$). Only the decays of the Z boson to charged leptons and leptonic W boson decays were considered as signal, leading to a final state topology characterized by the presence of three isolated leptons, at least two jets and missing transverse energy from the undetected neutrino. No evidence for an FCNC signal was found. An upper limit on the $t \to qZ$ branching ratio of $B(t \to qZ)$ <0.73% is set at the 95% confidence level [233]. Another analysis looks for FCNCs in $t \to cH$ with $H \to \gamma\gamma$ in 20 fb^{-1} of $t\bar{t}$ events at $\sqrt{s} = 9$ TeV, yielding a 95% C.L. limit of the tcH coupling of 0.17 (0.14 expected) [234].

D. Outlook

Top-quark physics at hadron colliders has developed into precision physics. Various properties of the top quark have been measured with high precision, where the LHC is about to or has already reached the precision of the Tevatron. Several $\sqrt{s}$-dependent physics quantities, such as the production cross-section, have been measured at several energies at the Tevatron and the LHC. Up to now, all measurements are consistent with the SM predictions and allow stringent tests of the underlying production mechanisms by strong and weak interactions. Given the very large event samples available at the LHC, top-quark properties will be further determined in $t\bar{t}$ as well as in electroweak single top-quark production. At the

Tevatron, the $t-$ and $s-$channels for electroweak single top-quark production have been measured separately. At the LHC, significant progress has been achieved and all the three relevant channels are expected to be independently accessible in the near future. Furthermore, $t\bar{t}\gamma$, $t\bar{t}Z$ and $t\bar{t}W$ associated production will provide further information on the top-quark electroweak couplings. At the same time various models of physics beyond the SM involving top-quark production are being constrained. With the upcoming LHC Run-II with twice the center-of-mass energy and much higher luminosity, top-quark physics has the potential to shed light on new aspects of and open questions in physics at the TeV scale.

References

CDF note references can be retrieved from `www-cdf.fnal.gov/physics/new/top/top.html`, and DØ note references from `www-d0.fnal.gov/Run2Physics/WWW/documents/Run2Results.htm` and ATLAS note references from `https://twiki.cern.ch/twiki/bin/view/AtlasPublic/TopPublicResults` and CMS note references from `https://twiki.cern.ch/twiki/bin/view/CMSPublic/PhysicsResultsTOP`.

1. M. Czakon, P. Fiedler and A. Mitov, Phys. Rev. Lett. **110**, 252004 (2013).
2. M. Cacciari *et al.*, JHEP **0809**, 127 (2008); N. Kidonakis and R. Vogt, Phys. Rev. **D78**, 074005 (2008); S. Moch and P. Uwer, Nucl. Phys. (Proc. Supp.) **B183**, 75 (2008); S. Moch and P. Uwer, Phys. Rev. **D78**, 034003 (2008); U. Langenfeld, S. Moch, and P. Uwer, Phys. Rev. **D80**, 054009 (2009); M. Beneke *et al.* Phys. Lett. **B690**, 483 (2010); M. Beneke *et al.*, Nucl. Phys. **B855**, 695 (2012); V. Ahrens *et al.*, Phys. Lett. **B703**, 135 (2011); M. Cacciari *et al.*, Phys. Lett. **B710**, 612 (2012).
3. The Tevatron Electroweak Working Group, For the CDF and DØ Collabs., `arXiv:1305.3929`.
4. S. Cortese and R. Petronzio, Phys. Lett. **B253**, 494 (1991).
5. S. Willenbrock and D. Dicus, Phys. Rev. **D34**, 155 (1986).
6. N. Kidonakis, Phys. Rev. **D83**, 091503 (2011).
7. N. Kidonakis, Phys. Rev. **D81**, 054028 (2010).

8. N. Kidonakis, Phys. Rev. **D82**, 054018 (2010).
9. T. Tait and C.-P. Yuan. Phys. Rev. **D63**, 014018 (2001).
10. M. Jeżabek and J.H. Kühn, Nucl. Phys. **B314**, 1 (1989).
11. I.I.Y. Bigi *et al.*, Phys. Lett. **B181**, 157 (1986).
12. A.H. Hoang *et al.*, Phys. Rev. **D65**, 014014 (2002).
13. K. Hagiwara, Y. Sumino, and H. Yokoya, Phys. Lett. **B666**, 71 (2008).
14. A. Czarnecki and K. Melnikov, Nucl. Phys. **B544**, 520 (1999); K.G. Chetyrkin *et al.*, Phys. Rev. **D60**, 114015 (1999).
15. S. Frixione, P. Nason, and B. Webber, JHEP **08**, 007 (2003); S. Frixione, P. Nason, and C. Oleari, JHEP **07**, 070 (2007); S. Frixione, P. Nason, and G. Ridolfi, JHEP **07**, 126 (2007).
16. S. Frixione *et al.*, JHEP **06**, 092 (2006); S. Frixione *et al.*, JHEP **08**, 029 (2008); S. Alioli *et al.*, JHEP **09**, 111 (2009); E. Re, Eur. Phys. J. C **71**, 1547 (2011); R. Frederix, E. Re, and P. Torrielli, JHEP **12**, 130 (2012).
17. S. Frixione and B.R. Webber, JHEP **02**, 029 (2002).
18. P. Nason, JHEP **04**, 040 (2004).
19. V.M. Abazov *et al.* (DØ Collab.), Phys. Lett. **B704**, 403 (2011).
20. T. Aaltonen *et al.* (CDF Collab.), CDF conference note 9913 (2009).
21. T. Aaltonen *et al.* (CDF Collab. and DØ Collab.), `arXiv:1309.7570`, submitted to Phys. Rev. D (2013).
22. ATLAS Collab., ATLAS-CONF-2011-121.
23. G. Aad *et al.* (ATLAS Collab.), JHEP **1205**, 059 (2012).
24. ATLAS Collab., ATLAS-CONF-2011-140.
25. ATLAS Collab., ATLAS-CONF-2012-024.
26. G. Aad *et al.* (ATLAS Collab.), Eur. Phys. J. **C73**, 2328 (2013).
27. G. Aad *et al.* (ATLAS Collab.), Phys. Lett. **B717**, 89 (2012).
28. ATLAS Collab., ATLAS-CONF-2012-031.
29. S. Chatrchyan *et al.* (CMS Collab.), Phys. Lett. **B720**, 83 (2013).
30. S. Chatrchyan *et al.* (CMS Collab.), JHEP **11**, 067 (2012).
31. S. Chatrchyan *et al.* (CMS Collab.), JHEP **1305**, 065 (2013).

32. S. Chatrchyan *et al.* (CMS Collab.), Phys. Rev. **D85**, 112007 (2012).
33. S. Chatrchyan *et al.* (CMS Collab.), Eur. Phys. J. **C73**, 2386 (2013).
34. ATLAS Collab., ATLAS-CONF-2012-149.
35. ATLAS Collab., ATLAS-CONF-2013-097.
36. CMS Collab., CMS-PAS-TOP-12-006.
37. CMS Collab., CMS-PAS-TOP-12-007.
38. V.M. Abazov *et al.* (DØ Collab.) Phys. Rev. Lett. **107**, 121802, (2011); D. Acosta *et al.* (CDF Collab.) Phys. Rev. Lett. **95**, 102002, (2005).
39. CMS Collab., CMS-PAS-TOP-12-035.
40. ATLAS Collab., ATLAS-CONF-2011-108.
41. V.M. Abazov *et al.* (DØ Collab.), Phys. Rev. **D67**, 012004 (2003).
42. T. Affolder *et al.* (CDF Collab.), Phys. Rev. **D64**, 032002 (2001).
43. T. Affolder *et al.* (CDF Collab.), Phys. Rev. Lett. **102**, 222003 (2009).
44. DØ Collab., D0-CONF-6379 (2013).
45. ATLAS Collab., ATLAS-CONF-2013-099 (2013).
46. S. Chatrchyan *et al.* (CMS Collab.), Eur. Phys. J. **C73**, 2339 (2013).
47. CMS Collab., CMS-PAS-TOP-12-027 (2013).
48. CMS Collab., CMS-PAS-TOP-12-028 (2013).
49. CMS Collab., CMS-PAS-TOP-12-042 (2013).
50. ATLAS Collab., ATLAS-CONF-2012-16 (2012).
51. ATLAS Collab., ATLAS-CONF-2012-155 (2012).
52. V.M. Abazov *et al.* (DØ Collab.), Phys. Rev. Lett. **103**, 092001 (2009); V.M. Abazov *et al.* (DØ Collab.), Phys. Rev. **D78**, 12005 (2008); V.M. Abazov *et al.* (DØ Collab.), Phys. Rev. Lett. **98**, 181802 (2007).
53. T. Aaltonen *et al.* (CDF Collab.), Phys. Rev. Lett. **103**, 092002 (2009); T. Aaltonen *et al.* (CDF Collab.), Phys. Rev. **D81**, 072003 (2010).
54. T. Aaltonen *et al.* (CDF Collab.), Phys. Rev. **D82**, 112005 (2010).
55. A. Heinson and T. Junk, Ann. Rev. Nucl. Part. Sci. **61**, 171 (2011).
56. Tevatron Electroweak Working Group, `arXiv:0908.2171v1 [hep-ex]`.

57. CDF Collab., CDF conference note 10793 (2012).
58. CDF Collab., CDF conference note 10979 (2013).
59. V.M. Abazov *et al.* (DØ Collab.), Phys. Rev. **D84**, 112001 (2011).
60. CDF Collab., CDF conference note 11015 (2013).
61. CDF Collab., CDF conference note 11025 (2013).
62. DØ Collab., FERMILAB-PUB-13-252-E, arXiv:1307.0731, submitted to Physics Letters B.
63. V.M. Abazov *et al.* (DØ Collab.), Phys. Lett. **B705**, 313 (2011).
64. G. Aad *et al.*, ATLAS Collab., Phys. Lett. **B717**, 330 (2012).
65. S. Chatrychan *et al.*, CMS Collab., JHEP **12**, 035 (2012).
66. ATLAS Collab., ATLAS-CONF-2012-056.
67. ATLAS Collab., ATLAS-CONF-2012-132.
68. CMS Collab., CMS-PAS-TOP-12-011.
69. ATLAS and CMS Collab., ATLAS-CONF-2013-098, CMS-PAS-TOP-12-002.
70. CMS Collab., CMS-PAS-TOP-13-001.
71. CMS Collab., CMS-PAS-TOP-12-038.
72. C.D. White *et al.*, JHEP **11**, 74 (2009).
73. S. Frixione *et al.*, JHEP **07**, 29 (2008).
74. G. Aad *et al.*, ATLAS Collab., Phys. Lett. **B716**, 142 (2012).
75. S. Chatrychan *et al.*, CMS Collab., Phys. Rev. Lett. **110**, 022003 (2012).
76. ATLAS Collab., ATLAS-CONF-2013-100.
77. CMS Collab., CMS-PAS-TOP-12-040.
78. ATLAS Collab., ATLAS-CONF-2011-118.
79. CMS Collab., CMS-PAS-TOP-11-003.
80. W. Hollik & D. Pagani Phys. Rev. **D84**, 093003 (2011).
81. W. Bernreuther & Z.G. Si, Phys. Rev. **D86**, 034026 (2012).
82. S. Jung, H. Murayama, A. Pierce, J.D. Wells, Phys. Rev. **D81**, 015004 (2010).
83. V.M. Abazov *et al.* (DØ Collab.), Phys. Rev. Lett. **100**, 142002 (2008).
84. T. Aaltonen *et al.* (CDF Collab.), Phys. Rev. Lett. **101**, 202001 (2008).
85. V.M. Abazov *et al.* (DØ Collab.), Phys. Rev. **D84**, 112005 (2011).

86. T. Aaltonen *et al.* (CDF Collab.), Phys. Rev. **D87**, 092002 (2013).
87. T. Aaltonen, *et al.* (CDF Collab.), Phys. Rev. **D83**, 112003 (2011).
88. ATLAS Collab., ATLAS-CONF-2013-078.
89. S. Chatrchyan *et al.* (CMS Collab.), Phys. Lett. **B717**, 129 (2012).
90. CMS Collab., CMS PAS TOP-12-033.
91. DØ Collab., DØ conference note 6381 (2013).
92. V.M. Abazov *et al.* (DØ Collab.), `arXiv:1308.6690`.
93. T. Aaltonen *et al.* (CDF Collab.), FERMILAB-PUB-13-309-E, `arXiv:1308.1120`.
94. ATLAS Collab., ATLAS-CONF-2012-057.
95. CMS Collab., CMS PAS TOP-12-010.
96. G. Aad *et al.* (ATLAS Collab.), Eur. Phys. J. **C72**, 2039 (2012).
97. F. Abe *et al.* (CDF Collab.), Phys. Rev. **D50**, 2966 (1994).
98. A. Abulencia *et al.* (CDF Collab.), Phys. Rev. **D73**, 032003 (2006).
99. ATLAS Collab., ATLAS-CONF-2013-046.
100. S. Chatrchyan *et al.* (CMS Collab.), JHEP **12**, 105 (2012).
101. T. Aaltonen *et al.* (CDF Collab.), Phys. Rev. Lett. **109**, 152003 (2012).
102. V.M. Abazov *et al.* (DØ Collab.), Phys. Rev. **D84**, 032004 (2011).
103. V.M. Abazov *et al.* (DØ Collab.), Nature, **429**, 638 (2004).
104. K. Kondo *et al.* J. Phys. Soc. Jpn. **G62**, 1177 (1993).
105. R.H. Dalitz and G.R. Goldstein, Phys. Rev. **D45**, 1531 (1992); Phys. Lett. **B287**, 225 (1992); Proc. Royal Soc. London **A445**, 2803 (1999).
106. V.M. Abazov *et al.* (DØ Collab.), Phys. Rev. **D75**, 092001 (2007).
107. L. Sonnenschein, Phys. Rev. **D73**, 054015 (2006).
108. ATLAS Collab., ATLAS-CONF-2013-077.
109. S. Chatrchyan *et al.* (CMS Collab.), Eur. Phys. J. **C72**, 2202 (2012).
110. B. Abbot *et al.* (DØ Collab.), Phys. Rev. **D60**, 052001 (1999); F. Abe *et al.* (CDF Collab.), Phys. Rev. Lett. **82**, 271 (1999).

111. CDF Collab., CDF conference note 10635 (2011).

112. A. Abulencia *et al.* (CDF Collab.), Phys. Rev. **D74**, 032009 (2006).

113. V.M. Abazov *et al.* (DØ Collab.), Phys. Rev. Lett. **107**, 082004 (2011).

114. CMS Collab., `arXiv:1307.4617`.

115. ATLAS Collab., ATLAS-CONF-2012-030.

116. T. Aaltonen *et al.* (CDF Collab.), Phys. Rev. **D88**, 011101, (2013).

117. T. Aaltonen *et al.* (CDF Collab.), Phys. Lett. **B698**, 371 (2011).

118. CMS Collab., CMS PAS TOP-12-030.

119. T. Aaltonen *et al.* (CDF Collab.), Phys. Rev. **D80**, 051104, (2009).

120. V.M. Abazov *et al.* (DØ Collab.) Phys. Rev. Lett. **100**, 192004, (2008); CMS Collab., `arxiv:1307.1907`;
V.M. Abazov *et al.* (DØ Collab.) Phys. Lett. **B703**, 422, (2011);
ATLAS Collab., ATLAS-CONF-2011-054;
S. Chatrchyan *et al.* (CMS Collab.), `arXiv:1307.1907`, submitted to Phys. Lett. B;
U. Langenfeld, S. Moch, and P. Uwer, Phys. Rev. **D80**, 054009 (2009).

121. ATLAS & CMS Collabs., ATLAS-CONF-2013-102, CMS PAS TOP-13-005.

122. CDF Collab., CDF conference note 10456 (2011), `arXiv:1112.4891`.

123. A.H. Hoang and J.W. Stewart, Nucl. Phys. Proc. Suppl. **185**, 220 (2008).

124. A. B. Galtieri, F. Margaroli, and I. Volobouev, Rept. on Prog. in Phys. **75**, 056201 (2012).

125. G. Aad *et al.* (ATLAS Collab.), Phys. Lett. **B716**, 1 (2012).

126. S. Chatrychyan *et al.* (CMS Collab.), Phys. Lett. **B716**, 30 (2012).

127. G. Degrassi, *et al.* `arXiv:1205.6497`.

128. S. Alekhin, A. Djouadi, and S. Moch., Phys. Lett. **B716**, 214, (2012).

129. T. Aaltonen *et al.* (CDF Collab.), Phys. Rev. **D87**, 052013 (2013).

130. V.M. Abazov *et al.* (DØ Collab.), Phys. Rev. **D84**, 052005 (2011).

131. G. Aad *et al.* (ATLAS Collab.), arXiv:1310.6527.
132. S. Chatrychyan *et al.* (CMS Collab.), JHEP **06**, 109 (2012).
133. CMS Collab., CMS-PAS-TOP-12-031.
134. G. Mahlon and S. Parke, Phys. Rev. **D53**, 4886 (1996); G. Mahlon and S. Parke, Phys. Lett. **B411**, 173 (1997).
135. G.R. Goldstein, in *Spin 96: Proceedings of the 12th International Symposium on High Energy Spin Physics,* Amsterdam, 1996, ed. C.W. Jager (World Scientific, Singapore, 1997), p. 328.
136. T. Stelzer and S. Willenbrock, Phys. Lett. **B374**, 169 (1996).
137. W. Bernreuther *et al.* Nucl. Phys. **B690**, 81 (2004).
138. CDF Collab., CDF conference note 10719 (2011).
139. CDF Collab., CDF conference note 10211 (2010).
140. V.M. Abazov *et al.* (DØ Collab.) Phys. Rev. Lett. **108**, 032004,2012.
141. V.M. Abazov *et al.* (DØ Collab.), Phys. Rev. Lett. **107**, 032001 (2011).
142. V.M. Abazov *et al.* (DØ Collab.), Phys. Lett. **B702**, 16 (2011).
143. G. Mahlon & S.J. Parke, Phys. Rev. **D81**, 074024,2010.
144. G. Aad *et al.* (ATLAS Collab.) Phys. Rev. Lett. **108**, 212001 (2012).
145. W. Bernreuther & Z.G. Si, Nucl. Phys. **B837**, 90 (2010).
146. ATLAS Collab., ATLAS-CONF-2013-101.
147. CMS Collab., CMS PAS TOP-12-004.
148. A. Falk and M. Peskin, Phys. Rev. **D49**, 3320 (1994).
149. T. Aaltonen *et al.* (CDF Collab.), arXiv:1308.4050.
150. V.M. Abazov *et al.* (DØ Collab.) Phys. Rev. **D85**, 091104R (2012).
151. G.L. Kane, G.A. Ladinsky, and C.P. Yuan, Phys. Rev. **D45**, 124 (1992).
152. A. Czarnecki, J.G. Korner, and J.H. Piclum, Phys. Rev. **D81**, 111503 (2010).
153. CDF and DØ Collab., Phys. Rev. **D85**, 071106 (2012).
154. CDF Collab., Phys. Rev. **D87**, 031103 (2013).
155. ATLAS Collab., JHEP **1206**, 088 (2012).
156. CMS Collab., CMS-PAS-TOP-11-020, CERN-PH-EP/2013-133, arXiv:1308.3879, submitted to JHEP.

157. ATLAS and CMS Collab., ATLAS-CONF-2013-033, CMS-PAS-TOP-11-025.
158. CMS Collab., CMS-PAS-TOP-13-008.
159. CMS Collab., CMS-PAS-TOP-12-020.
160. D. Choudhury, T.M.P. Tait, and C.E.M. Wagner, Phys. Rev. **D65**, 053002 (2002).
161. D. Chang, W.F. Chang, and E. Ma, Phys. Rev. **D59**, 091503 (1999), Phys. Rev. **D61**, 037301 (2000).
162. V.M. Abazov *et al.* (DØ Collab.), Phys. Rev. Lett. **98**, 041801 (2007).
163. CDF Collab., `arXiv:1304.4141`, submitted to Phys. Rev. D (2013).
164. ATLAS Collab., CERN-PH-EP-2013-056, `arXiv:1307.4568`, submitted to JHEP (2013).
165. CMS Collab., CMS-PAS-TOP-11-031.
166. T. Aaltonen *et al.* (CDF Collab.), Phys. Rev. **D84**, 031104 (2011).
167. ATLAS Collab., ATLAS-CONF-2011-153.
168. S. Chatrchyan *et al.* (CMS Collab.), Phys. Rev. Lett. **110**, 172002 (2013).
169. ATLAS Collab., ATLAS-CONF-2012-126.
170. S.P. Martin, `arXiv:9709356` (1997).
171. C.T. Hill, Phys. Lett. **B266**, 419 (1991).
172. C.T. Hill, Phys. Lett. **B345**, 483 (1995).
173. C. Zhang and S. Willenbrock, Phys. Rev. **D83**, 034006 (2011).
174. J. A. Aguilar-Saavedra,Nucl. Phys. **B843**, 638 (2011).
175. V. Barger, T. Han, and D. G. E. Walker, Phys. Rev. Lett. **100**, 031801 (2008).
176. D. Choudhury *et al.*, Phys. Lett. **B657**, 69 (2007).
177. R. Frederix and F. Maltoni, JHEP **01**, 047 (2009).
178. ATLAS Coll. ATLAS-CONF-2012-130.
179. ATLAS Coll. ATLAS-CONF-2012-050.
180. G. Aad *et al.* (ATLAS Coll.), JHEP **1204**, 069 (2012).
181. T. Aaltonen (CDF Collab.), Phys. Rev. **D84**, 072004 (2011).
182. T. Aaltonen (CDF Collab.), Phys. Rev. Lett. **110**, 121802 (2013).
183. DØ Collab., FERMILAB-PUB-05/9-E, submitted to Phys. Rev. Lett.

184. T. Aaltonen (CDF Collab.), Phys. Rev. **D84**, 072003 (2011).
185. A. Altheimer, *et al.* , J. Phys. G **39**, 063001 (2012).
186. S. Chatrchyan *et al.* (CMS Collab.), Phys. Rev. **D87**, 072002 (2013).
187. S. Chatrchyan *et al.* (CMS Collab.), JHEP **1212**, 015 (2012).
188. S. Chatrchyan *et al.* (CMS Collab.), `arXiv:1309.2030`, submitted to Phys. Rev. Lett..
189. G. Aad *et al.* (ATLAS Collab.), Phys. Rev. **D88**, 012004 (2013).
190. ATLAS Collab., ATLAS-CONF-2013-052.
191. G. Aad *et al.* (ATLAS Collab.), JHEP **1301**, 116 (2013).
192. T. Plehn *et al.*, JHEP **1010**, 078 (2010).
193. ATLAS Collab., ATLAS-CONF-2012-096.
194. ATLAS Collab., ATLAS-CONF-2013-056.
195. ATLAS Collab., ATLAS-CONF-2013-018.
196. ATLAS Collab., ATLAS-CONF-2013-051.
197. CMS Collab., CMS-PAS-TOP-12-019.
198. G. Aad *et al.* (ATLAS Collab.), Phys. Rev. Lett. **108**, 041805 (2012).
199. CMS Collab., CMS-PAS-TOP-12-021.
200. ATLAS Collab., ATLAS-CONF-2013-063.
201. G. Aad *et al.* (ATLAS Collab.), Phys. Lett. **B712**, 351 (2012).
202. A. Heister *et al.* (ALEPH Collab.), Phys. Lett. **B543**, 173 (2002); J. Abdallah *et al.* (DELPHI Collab.), Phys. Lett. **B590**, 21 (2004); P. Achard *et al.* (L3 Collab.), Phys. Lett. **B549**, 290 (2002); G. Abbiendi *et al.* (OPAL Collab.), Phys. Lett. **B521**, 181 (2001).
203. F.D. Aaron *et al.* (H1 Collab.), Phys. Lett. **B678**, 450 (2009).
204. H. Abramowics *et al.* (ZEUS Collab.), Phys. Lett. **B708**, 27 (2012).
205. M. Beneke *et al.*, `hep-ph/0003033`, in *Proceedings of 1999 CERN Workshop on Standard Model Physics (and more) at the LHC*, G. Altarelli and M.L. Mangano eds.
206. V.F. Obraztsov, S.R. Slabospitsky, and O.P. Yushchenko, Phys. Lett. **B426**, 393 (1998).
207. T. Carli, D. Dannheim, and L. Bellagamba, Mod. Phys. Lett. **A19**, 1881 (2004).

208. ATLAS Collab., ATLAS-CONF-2011-087.
209. ATLAS Collab., ATLAS-CONF-2011-123.
210. CMS Collab., CMS-PAS-TOP-10-007.
211. CMS Collab., CMS-PAS-EXO-11-055.
212. CMS Collab., CMS-PAS-EXO-11-0006.
213. F. Abe *et al.* (CDF Collab.), Phys. Rev. Lett. **79**, 357 (1997);
T. Affolder *et al.* (CDF Collab.), Phys. Rev. **D62**, 012004 (2000).
214. B. Abbott *et al.* (DØ Collab.), Phys. Rev. Lett. **82**, 4975 (1999);
V.M Abazov *et al.* (DØ Collab.), Phys. Rev. Lett. **88**, 151803 (2002).
215. A. Abulencia *et al.* (CDF Collab.), Phys. Rev. Lett. **96**, 042003 (2006).
216. T. Aaltonen *et al.* (CDF Collab.), Phys. Rev. Lett. **103**, 101803 (2009).
217. V.M. Abazov *et al.* (DØ Collab.), Phys. Rev. **D80**, 071102 (2009).
218. V.M. Abazov *et al.* (DØ Collab.), Phys. Lett. **B682**, 278 (2009).
219. V.M. Abazov *et al.* (DØ Collab.), Phys. Rev. **D80**, 051107 (2009).
220. V.M. Abazov *et al.* (DØ Collab.), Phys. Rev. **D80**, 071102 (2009).
221. ATLAS Collab., ATLAS-CONF-2011-094.
222. ATLAS Collab., ATLAS-CONF-2011-138.
223. ATLAS Collab., ATLAS-CONF-2011-151.
224. ATLAS Collab., ATLAS-CONF-2011-154.
225. V.M. Abazov *et al.* (DØ Collab.), Phys. Rev. Lett. **102**, 092002 (2009).
226. V.M. Abazov *et al.* (DØ Collab.), DØ conference note 5838 (2009).
227. V.M. Abazov *et al.* (DØ Collab.), `arXiv:1110.4592`, submitted to Phys.Lett.B.
228. ATLAS Collab., ATLAS-CONF-2013-032.
229. T. Aaltonen *et al.* (CDF Collab.), Phys. Rev. Lett. **101**, 192002 (2009).
230. V.M. Abazov *et al.* (DØ Collab.), Phys. Lett. **B701**, 313 (2011).
231. V.M. Abazov *et al.* (DØ Collab.), Phys. Lett. **B693**, 81 (2010).

232. CMS Collab., CMS-PAS-TOP-12-037.
233. G. Aad *et al.* (ATLAS Collab.), JHEP **1209**, 139 (2012).
234. ATLAS Collab., ATLAS-CONF-2012-081.